

Utilization of CO₂ in High Performance Building and Infrastructure Products

Final Report

Covering the period October 1, 2010 – November 15, 2015

WORK PERFORMED UNDER AGREEMENT DE-FE0004222

SUBMITTED BY
Solidia Technologies, Inc.
11 Colonial Drive
Piscataway, NJ 08854
June 27, 2016

PRINCIPAL INVESTIGATOR
Nicholas DeCristofaro
908-315-5901
<ndecristofaro@solidiatech.com>

SUBMITTED TO
U.S. Department of Energy
National Energy Technology Laboratory
Mary (Kylee) Rice
304-285-4445
<Mary.Rice@netl.doe.gov>

Disclaimer

This report was prepared as an account of work sponsored by an agency of the United States Government. Neither the United States Government nor any agency thereof, nor any of their employees, makes any warranty, express or implied, or assumes any legal liability or responsibility for the accuracy, completeness, or usefulness of any information, apparatus, product, or process disclosed, or represents that its use would not infringe privately owned rights. Reference herein to any specific commercial product, process, or service by trade name, trademark, manufacturer, or otherwise does not necessarily constitute or imply its endorsement, recommendation, or favoring by the United States Government or any agency thereof. The views and opinions of authors expressed herein do not necessarily state or reflect those of the United States Government or any agency thereof.

Table of Contents

	<u>Page</u>
Title Page	1
Table of Contents	3
Executive Summary	6
1. Project Description	8
2. Market Study	11
3. Technical Evaluation	13
A. Background	13
B. Subtasks 3.1 to 3.9	14
<i>i. Control of Mineral Particle Size</i>	14
<i>ii. Methods to Measure Mineral Carbonation Rate and Yield</i>	15
<i>iii. Mineral Carbonation Reaction Rate Dependence on Particle Size</i>	18
<i>iv. Mechanical Properties of Pressed and Carbonated Pellets</i>	20
<i>v. Summary</i>	22
C. Subtasks 3.10 to 3.12	23
<i>i. Subtask 3.10 (Revised) Investigate Water Distribution Changes During Drying</i>	23
<i>ii. Subtask 3.11 (New) Investigate Water Distribution Changes During Curing</i>	27
<i>iii. Subtask 3.12 (New) Find the Optimum Curing Conditions</i>	32
4. Demonstration of Commercial Application	40
A. Background	40
B. Subtasks 4.1 to 4.3	41
<i>i. Subtask 4.1 Demonstrate the basic performance of Solidia Cement</i>	41
<i>ii. Subtask 4.2 Demonstrate the utility of Solidia Cement and initiate its commercialization in precast operations and applications</i>	44
<i>iii. Subtask 4.3 Develop, optimize and implement curing processes required for cost effective and scalable manufacturing of Solidia Concrete for target precast concrete manufacturers</i>	48
5. Greenhouse Gas and non-GHG Impacts	59
6. Scientific Achievements	64
7. Overall Conclusions	66

LIST OF FIGURES

Figure 1. (a) As-received wollastonite (NYAD 400), (b) powder milled for almost 5 h with 1 mm zirconia balls, and (c) magnified image of (b)

Figure 2. (a) Calculated mean particle size and (b) specific surface area of milled powder versus milling time

Figure 3. (a) The Bruker D8 Discover X-Ray Diffraction unit and (b) the in-situ reaction cell

Figure 4. (a) XRD patterns of NYAD 400 powder at 0, 8, and 17 hours of reaction, (b) the intensity map of the entire reaction process (c) percentage of evolved phases versus reaction time

Figure 5. a) Remspec FTIR setup, b) sample with probe

Figure 6. (a) Contour plot of in-situ FT-IR measurement of wollastonite during reaction with the IR spectra at different reaction times (right) and the absorbance trend lines for different wavenumbers (top). (b) the IR spectra of wollastonite during reaction

Figure 7. (a) Trend lines representing the peak intensities of carbonate, silica, and silicate over time, (b) the calculated mole fraction of carbonates from FTIR data and those obtained from the TGA analysis

Figure 8: TGA of reacted NYAD 5000 powder

Figure 9. (a) Carbonation yields of (a) powders with various particle sizes and (b) nano-size milled NYAD 400 with and without heat treatment

Figure 10. The effect of (a) mean particle size and (b) specific surface area of calcium silicate powders on carbonation yield. Powders were carbonated for 19 h at 90°C and 20 psi gauge pressure. The carbonation yield of synthetic wollastonite is shown by red dots

Figure 11. The carbonation yields of as-received mineral and synthetic wollastonites versus reaction time at (a) 70°C and (b) 50°C. (c) The effect of temperature on carbonation yields of these powders (19 h and 20 psig)

Figure 12. (a) Carbonation yield and (b) compressive strength of NYAD 400 pellet reacted under 20 psig versus temperature. (c) Carbonation yield and (d) compressive strength of NYAD 400 pellet reacted under 20 psig versus time. (e) Carbonation yield and (f) compressive strength of NYAD 400 pellets reacted for 19 h at 90°C versus pressure gauge

Figure 13. Typical drying curves for constant-rate and falling-rate periods

Figure 14. Paver drying curves

Figure 15. Drying curves of a lightweight block

Figure 16. Aerated green sample drying curves

Figure 17. Pictures of front development in various types of Solidia Concrete product cross-sections
(Top) Hollow-core slab cross-section measuring 4 feet wide x 8 inches high. (Middle) Railroad Tie cross-section measuring 12 inches x 8 inches. (Bottom left) Cylinder cross-section, 4-inch diameter x 12 inches long. (Bottom right) 2-inch cube cut from a larger piece of aerated concrete

Figure 18. Solidia Concrete hollow-core slab test bed

Figure 19. Thermocouple responses during the curing process

Figure 20. Thermocouple responses due to heating alone

Figure 21. Thermocouple responses due only to heating and drying together

Figure 22. Endothermal effect of drying as function of time (blue) and exothermal effect of carbonation as a function of time (Red) during curing of Solidia Concrete

Figure 23. Time evolution of the relative humidity envelope during the curing of a hollow-core slab

Figure 24. Side view (top) and top view (bottom) of gas flow pattern

Figure 25. Relative humidity contours within the curing chamber

Figure 26. Model frequency distribution of water vapor mole fraction

Figure 27. Measured frequency distribution of water vapor mole fraction

Figure 28. Columbia block and paver press

Figure 29. Unevenly dried Solidia Concrete CMUs

Figure 30. Contour plot of relative humidity throughout the chamber with modifications

Figure 31. Evenly dried Solidia Concrete CMUs

Figure 32. Solidia Concrete railroad tie before (left) and after (right) CO₂-curing

Figure 33. Railroad tie loaded onto curing cart (left) and sealed prior to carbonation (right)

Figure 34. Optimized railroad tie curing profile

Figure 35: CO₂-curing humidity envelopes for hollow-core slab extruded with 5.5 (left) and 4.1 (right) weight % water in the concrete mix

Figure 36. Base case for an 800 minute CO₂-curing exposure

Figure 37. Influence of CO₂ circulation speed and the gas-flow reversal period on curing time

Figure 38. Normalized mass gain of Whitehall cement and synthetic carbonatable phases carbonated at 30°C, 60°C and 90°C

Figure 39. Normal weight CMUs on a curing rack

Figure 40. Flat roof tile in two colors

Figure 41. Hardface paver (left) and retaining wall blocks (right)

Figure 42. Paver and Block Manufacturer #2's curing chambers with roll-down doors

Figure 43. Magnesium oxide board installation

Figure 44. Sandblasting

Figure 45. Spray coating
Figure 46. Completed door
Figure 47. Door carriage installed
Figure 48. Door manipulation design
Figure 49. CFD model for Paver and Block Manufacturer #2
Figure 50. Vertical inlet ductwork installed
Figure 51. Inlet and outlet headers installed
Figure 52. Gas conditioning system - heater
Figure 53. Gas conditioning system - view from heater
Figure 54. Gas conditioning system - view from side opposite heater
Figure 55. Temporary CO₂ tank
Figure 56. Solidia Cement silo installed (left)
Figure 57. Commissioning Run #1 production line
Figure 58. Chamber loading
Figure 59. Chamber temperature profile
Figure 60: Chamber RH profile
Figure 61. Schematic of the loss on ignition process used to measure CO₂ sequestration in a paver

LIST OF TABLES

Table 1. Milling conditions
Table 2. TGA carbonation yields
Table 3. Specific surface area and mean particle size of various calcium silicates.
Table 4. Physical and mechanical properties of various wollastonite materials
Table 5. Parameters used in the CFD model
Table 6. Width of frequency distribution of water vapor mole fraction
Table 7. Average elemental composition as measured by X-Ray Fluorescence (XRF)
Table 8. Average clinker phase composition as measured by X-Ray Diffraction (XRD)
Table 9. Particle statistics of Whitehall milled cement as determined by averaging particle size measurements throughout the grinding operation
Table 10. Specific surface area measurements of materials subjected to carbonation testing
Table 11. Composition of experimental mortar
Table 12. Results of the mortar cube evaluation
Table 13. Experimental concrete mixture proportions
Table 14. Results of the mortar cube evaluation
Table 15. Timeline for moving forward on ASTM codes
Table 16. Benefit summary of Solidia Concrete
Table 17. Potential value-adding attributes of Solidia's Cement and Concrete Technologies
Table 18. Pro forma Income Statement for Concrete Paver Manufacturer Converting to Solidia Technologies (000's)
Table 19. Key System Cost Comparisons Per Ton of Cement
Table 20. Compressive Strength Results for Pavers Produced During Commissioning Run #1
Table 21. Hollow Core CO₂ sequestration measured by Loss on Ignition (LOI)
Table 22. Carbon footprint for Paver and Block Manufacturer #2 for Solidia Cement and Solidia Concrete compared to Portland cement and concrete

Executive Summary

The overall objective of DE-FE0004222 was to demonstrate that calcium silicate phases, in the form of either naturally-occurring minerals or synthetic compounds, could replace Portland cement in concrete manufacturing. The calcium silicate phases would be reacted with gaseous CO₂ to create a carbonated concrete end-product. If successful, the project would offer a pathway to a significant reduction in the carbon footprint associated with the manufacture of cement and its use in concrete (approximately 816 kg of CO₂ is emitted in the production of one tonne of Portland cement).

In the initial phases of the Technical Evaluation, Rutgers University teamed with Solidia Technologies to demonstrate that natural wollastonite (CaSiO₃), milled to a particle size distribution consistent with that of Portland cement, could indeed fit this bill. The use of mineral wollastonite as a cementitious material would potentially eliminate the CO₂ emitted during cement production altogether, and store an additional 250 kg of CO₂ during concrete curing. However, it was recognized that mineral wollastonite was not available in volumes that could meaningfully impact the carbon footprint associated with the cement and concrete industries.

At this crucial juncture, DE-FE0004222 was redirected to use a synthetic version of wollastonite, hereafter referred to as Solidia Cement™, which could be manufactured in conventional cement making facilities. This approach enables the new cementitious material to be made using existing cement industry raw material supply chains, capital equipment, and distribution channels. It would also offer faster and more complete access to the concrete marketplace.

The latter phases of the Technical Evaluation, conducted with Solidia Cement made in research rotary kilns, would demonstrate that industrially viable CO₂-curing practices were possible. Prototypes of full-scale precast concrete products such as pavers, concrete masonry units, railroad ties, hollow-core slabs, and aerated concrete were produced to verify the utility of the CO₂-curing process. These products exhibited a range of part dimensions and densities that were representative of the precast concrete industry.

In the subsequent Demonstration of Commercial Development phase, the characteristics and performance of Solidia Cement made at a LafargeHolcim cement plant were established. This Solidia Cement was then used to demonstrate the CO₂-curing process within operating concrete plants. Pavers, concrete masonry units and roofing tiles were produced according to ASTM and manufacturer specifications. A number of attractive manufacturing economies were recognized when Solidia Cement-based concrete parts were compared to their Portland cement based counterparts. These include reduced raw materials waste, reduced dependence on admixtures to control efflorescence, shorter curing time to full concrete strength, faster equipment clean-up, reduced equipment maintenance, and improved inventory management. ***These economies make the adoption of the Solidia Cement / CO₂-curing process attractive even in the absence of environmental incentives.***

The culminating activity of the Demonstration of Commercial Development phase was the conversion of 10% of the manufacturing capacity at a concrete paver and block company from Portland cement-based products to Solidia Cement-based products.

The successful completion of the Demonstration of Commercial Development phase clearly illustrated the environmental benefits associated with Solidia Cement and Solidia Concrete technologies. The industrial production of Solidia Cement, as a low-lime alternative to traditional Portland cement, reduces CO₂ emissions at the cement kiln from 816 kg of CO₂ per tonne of Portland cement clinker to 570 kg per tonne of Solidia Cement clinker. Industrial scale CO₂-curing of Solidia Concrete sequestered a net of 183 kg of CO₂ per tonne of Solidia Cement used in concrete pavers. Taken together, these two effects reduced the CO₂

footprint associated with the production and use of cement in concrete products by over 50% (a reduction of 430 kg of CO₂ per tonne of cement).

Applied at the first commercial Solidia Concrete manufacturing site, the two effects will combine to reduce the CO₂ footprint associated with the production and use of cement by over 10,000 tonnes per year. When applied across the precast concrete industry in the U.S., it is estimated that the CO₂ footprint will be reduced by 8.6 million tonnes per year (20 million tonnes of cement used in precast concrete x 430 kg of CO₂ per tonne of cement). **Applied across the entire concrete industry in the U.S., it is expected that 43 million tonnes of CO₂ will be avoided per year (100 million tonnes of cement used in all concrete x 430 kg of CO₂ per tonne of cement).**

1. Project Description

Task 1.0 Project Management and Reporting

Project Management decisions made in the course of the DE-FE0004222 program are described in the subsections below.

Task 2.0: Business Evaluation

This task was initially completed in September 2011. A revised perspective of the potential business implications was considered in March 2013 and included in the decision to revise Technical Evaluation Subtask 3.10 and add new Subtasks 3.11 and 3.12. This perspective was also considered when creating the new as Task 4, Demonstration of Commercial Application.

Task 3.0 Technical Evaluations

In the initial phases of the Technical Evaluation, Rutgers University teamed with Solidia Technologies to explore the viability of mineral wollastonite (CaSiO_3) as a cementitious material in the production of a CO_2 -cured concrete. Subtasks 3.1 through 3.9, completed in December 2012, studied the impact of wollastonite particle size on its CO_2 -reaction rate and reaction extent. This work included the acquisition of milling and instrumentation capabilities designed to improve the reaction rate of wollastonite.

Brief descriptions of the specific activities associated with Subtasks 3.1 through 3.9 are offered below:

Subtask 3.1 Acquire, install, and commission grinding mill

The mill was ordered and installed along with the required utilities. Acceptance testing was performed.

Subtask 3.2 Control mineral particle size using the grinding mill

The mill was used to reduce the particle size under a range of conditions and correlate them with particle size.

Subtask 3.3 Acquire, install, and commission HP-TGA

The HP-TGA was ordered and installed along with the required utilities. Acceptance testing was performed.

Subtask 3.4 Use TGA-HP to study reaction rate and carbonation yield dependence on temperature and pressure

The reaction rate and amount of carbonate formed were measured as a function of CO_2 pressure and reaction temperature.

Subtask 3.5 Study reaction rate and carbonation yield dependence on particle size using the grinding mill and TGA-HP

The reaction rate and carbonation yield were plotted as a function of temperature and pressure for powders having different particle sizes. From these plots the ideal particle size for carbonation based on pressure and temperature was identified.

Subtask 3.6 Study reaction rate and carbonation yield dependence on temperature and pressure for pressed pellets made from powder having ideal particle size

Using the ideal particle size determined in subtask 3.5, a compact was made by powder consolidation and reacted with CO_2 in an autoclave. The reaction rate was then be plotted as a function of temperature and pressure. Using the ideal particle size determined in Subtask 3.5, a compact was be made and the carbonation yield determined. The carbonation yield was then be plotted as a function temperature and pressure to identify the ideal particle size for carbonation based on pressure and temperature data.

Subtask 3.7 Perform energy study for comminution using grinding mill

The energy expended per ton of raw material will be measured to determine the most efficient milling conditions.

Subtask 3.8 Measure compressive and tensile strength of carbonated samples

The compressive strength of samples was measured using ASTM methods.

Subtask 3.9 Determine best raw material formulation based on chemistry, mechanical strength, carbonation yield, reaction rate, energy cost and CO₂ footprint

The best process for making building panels was identified with consideration to raw materials chemistry, the process used to make the material, the chemical and physical characteristics of the carbonate product, the mechanical properties, and the energy and CO₂ footprint.

DECISION POINT – Prior to commencing with Subtask 3.10 in 2013, the NETL Project Officer assessed the prior completed tasks in order to make a go-no go decision prior to proceeding with the original Subtask 3.10.

A brief description of the specific activities associated with the original Subtask 3.10 is offered below:

Subtask 3.10 (Original) Design, acquire, install and commission autoclave, to scale-up process and make prototype panels

Based on the best process to make building panels, a reactor that can scale up the size of the panels to 1 ft x 1 ft as well as process multiple panels will be designed, built and commissioned.

Working together, the NETL Program Officer and Solidia Technologies opted to revise Subtask 3.10, and add new Subtasks 3.11 and 3.12. This decision was based on the fact that mineral wollastonite was not available in sufficient volumes to meaningfully impact the carbon footprint of the concrete industry. The factors weighed in this decision are described in Section 2 Business Evaluation. A revised Project Management Plan was drafted and submitted to the NETL program officer in March 2013. Work according to the new Subtasks 3.10 through 3.12 was commenced on April 1, 2013 and completed in June 2014.

The new Subtasks replaced mineral wollastonite with a synthesized version of wollastonite. The synthesized version, hereafter referred to as Solidia Cement™, can be made in conventional cement making facilities. Additionally, the concrete forms produced and tested in these new subtasks represented actual concrete products, ranging from pavers to railroad ties to hollow-core slabs. These products exhibit a range of concrete part dimensions and densities that are representative of the entire Portland cement concrete industry. The focus of the work was the study of the effects of sample geometry, density and internal water distribution on the Solidia Cement reaction rate, during both the drying and curing phases of the concrete production process.

Brief descriptions of the specific activities associated with Subtasks 3.10 through 3.12 are offered below:

Subtask 3.10 (Revised) Investigate water distribution changes in the sample during drying

Drying curves were generated and analyzed for Solidia Concrete™ samples of various densities and sizes. Raw materials Solidia Cement, sand, aggregate and other necessary compounds and chemicals) and molds for three product forms were purchased. The product forms to be tested were a high-density concrete paver, a medium-density concrete masonry unit, and a low-density aerated concrete form.

Subtask 3.11 (new) Investigate water distribution changes in the sample during curing

Using the information generated, and the analytical equipment acquired in Subtask 3.10, drying curves were generated for Solidia Concrete samples during curing with CO₂. CO₂ curing times were determined based on the drying rates measured in the previously described experiments. Carbonation rates, carbonation yields, residual water contents and residual water gradients were evaluated in an effort to optimize the CO₂-curing process.

Subtask 3.12 (new) Find the optimum reaction conditions for given sample size, geometry and density

Using the information generated in Subtasks 3.10 and 3.11, optimum reaction conditions were identified for concrete pavers, concrete masonry units, railroad ties and hollow core slabs. The reaction conditions included the initial water content in the uncured part, the water distribution within the uncured part, the curing temperature and humidity levels, and the CO₂ gas flow rates. Each resulting CO₂-cured product form was evaluated according to the full commercial process and product specifications for the Portland cement concrete version of that part.

Task 4.0 Demonstration of Commercial Application

At the successful completion of Task 3.0 Technical Evaluation, the NETL Program Officer and Solidia Technologies recommended continuing the program with a purpose of laying the technology foundation for the commercial development of carbonated concrete products. This work focused on a characterization of Solidia Cement produced at a commercial cement plant, and the subsequent production of carbonated concrete parts from that cement. It concluded with the demonstration that the CO₂-curing process could indeed be considered as a cost effective and scalable manufacturing process for the target precast Solidia Concrete applications.

Brief descriptions of the specific activities associated with Subtasks 4.1 through 4.3 are offered below:

Subtask 4.1: Demonstrate the basic performance of Solidia Cement produced at a commercial cement plant (LafargeHolcim in Whitehall, PA).

The chemistry, mineralogy (phase content), particle size distribution, particle surface area and reactivity with CO₂ for Solidia Cement from Whitehall were analyzed and compared to previous variants of Solidia Cement. Using the information generated in Subtask 3.12, the Solidia Cement was evaluated in CO₂-cured mortar and concrete forms. This included production and testing according to ASTM C109 and C1437 for mortar cubes, and ASTM C39 for concrete cylinders.

Subtask 4.2: Demonstrate the utility of Solidia Cement and initiate its commercialization in precast concrete operations and applications.

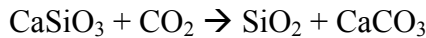
Target precast concrete applications were identified in association with US-based concrete manufacturers willing to participate in this effort. For each concrete manufacturer, prototype CO₂-curing reactors were installed with the capability to produce full-sized concrete parts. At each site, concrete parts made with Solidia Cement were prepared as per the curing standards developed in Subtask 3.12 and tested according to the full commercial process and product specifications for the Portland cement concrete version of that part. Note that the concrete manufacturing trials conducted in the execution of Subtask 4.2 are referred to as Phase 1 trials.

Subtask 4.3: Develop, optimize and implement curing processes required for cost effective and scalable manufacturing of Solidia Concrete for target precast concrete manufacturers.

Using the information generated in Subtask 4.2, the production economics and commercial viability of the CO₂-curing process at each target, precast concrete manufacturing site were analyzed. This effort included calculation of the capital investment needed to convert the manufacturer's existing curing system into a CO₂-curing system as well as the overall production costs. At a selected manufacturing site, approximately 10% of the existing curing system capacity was converted to CO₂-curing capability. Solidia Cement based concrete product forms were then manufactured and tested according to the full commercial process and product specifications for the Portland cement concrete version of that part. At the selected site, the production economics were verified. CO₂ stored per tonne concrete and overall the CO₂ reduction per tonne of Solidia Cement deployed were assessed for key product forms. Note that the concrete manufacturing trials conducted in the execution of Subtask 4.3 are referred to as Phase 3 trials.

2. Market Study

At the outset of DE-FE0004222 “Utilization of CO₂ in High Performance Building and Infrastructure Products”, it was projected that mineral wollastonite (CaSiO₃) would serve as a cementitious material to replace Portland cement in concrete construction materials. Traditional concrete cures and hardens by way of a reaction between Portland cement and water. By contrast, a wollastonite-based concrete would cure and harden by way of a reaction between CaSiO₃ and gaseous CO₂ in the presence of water, converting the wollastonite to a porous form of SiO₂, and precipitating CaCO₃ within the pores of the concrete. The reaction would proceed as follows:



By this mechanism, wollastonite can capture and permanently store up to 40% of its weight in CO₂. The precipitation of stable CaCO₃ in the form of calcite would bond together the sand and aggregate components of the concrete to form strong, rigid structures.

The environmental impact associated with the replacement of Portland cement with mineral wollastonite is potentially profound. The synthesis of one tonne of Portland cement results in the emission of 816 kg of CO₂. This is a result of the decomposition of limestone and the burning of coal integral to cement manufacturing. Using mineral wollastonite would eliminate these emissions. Additionally, 250 kg of CO₂ would be permanently stored in the carbonated concrete product for each tonne of mineral wollastonite used as a cementitious material.

Thus, the carbon footprint associated with the manufacturing and use of one tonne of cement could be reduced by 1,066 kg (816 kg of CO₂ emissions avoided at the cement plant plus 250 kg of CO₂ stored during concrete curing).

However, only about 100,000 tonnes of wollastonite is mined in North America each year. If this entire volume of wollastonite was used as a cementitious material replacing Portland cement, then the CO₂ footprint associated with the manufacturing and use of cement would be reduced by 106,600 tonnes.

By comparison, over 100,000,000 tonnes of Portland cement are manufactured and used in the U.S. each year.

DE-FE0004222, Task 2.0 (Business Evaluation) studied the US market for high-end countertop materials as a potential launch application for a wollastonite-based concrete product. This market, comprised of natural stone (eg. granite, marble, onyx), engineered stone and solid concrete, is scaled appropriately for the use of wollastonite as a cementitious material. High-end countertop applications in the US total 162 million ft² of surface area per year (equivalent to approximately 40 million ft³, or 3 million tonnes of concrete). Assuming that a high performance concrete would contain 20 wt.% cement, this market would require 600,000 tonnes of wollastonite. In the long run, however, this demand would easily exceed the annual North American production.

As a result of this realization, the NETL Program Officer and Solidia Technologies collaborated to change the direction of DE-FE0004222. Rather than continuing with the use of mineral wollastonite as a cementitious material in a CO₂-cured concrete, a synthetic version of wollastonite was adopted. This synthetic version, referred to as Solidia Cement, could be manufactured in conventional cement making facilities. This approach enables the new cementitious material to be made using existing cement industry raw material supply chains, capital equipment, and distribution channels. More importantly, by preserving

the Portland cement infrastructure rather than competing with it, this approach would permit a faster adoption in, and a more complete penetration of, the concrete industry.

From that point forward, DE-FE0004222 would focus on the use of Solidia Cement, first made in research rotary kilns and later made at a LafargeHolcim cement manufacturing facility. The latter portion of the Technical Evaluation, and the subsequent Demonstration of Commercial Development, would demonstrate that a variety of precast concrete products, such as pavers, concrete masonry units, railroad ties, hollow core slabs and aerated concrete, could be made with Solidia Cement.

The manufacture of Solidia Cement in a conventional cement plant, reduces both limestone and coal consumption by 30%. Thus, CO₂ emissions are reduced from 816 kg per tonne of Portland cement to 570 kg per tonne of Solidia Cement. As in the mineral wollastonite case described above, 250 kg of CO₂ will be stored during concrete curing for each tonne of Solidia Cement.

The implications of this change are profound. Solidia Cement, applied to the precast concrete industry (~20% of the total concrete industry), offers the potential to reduce the CO₂ footprint associated with cement manufacturing and use by 8.6 million tonnes per year. If applied to the entire concrete industry (precast plus cast-in-place), this benefit increases to 43 million tonnes.

3. Technical Evaluation

3.A. Background

At the outset of DE-FE0004222 “Utilization of CO₂ in High Performance Building and Infrastructure Products”, it was projected that mineral wollastonite (CaSiO₃) would serve as a cementitious material to replace Portland cement in concrete construction materials. Traditional concrete cures and hardens by way of a reaction between Portland cement and water. By contrast, a wollastonite-based concrete would cure and harden by way of a reaction between CaSiO₃ and gaseous CO₂ in the presence of water, converting the wollastonite to a porous form of SiO₂, and precipitating CaCO₃ within the pores of the concrete. The reaction would proceed as follows:



By this mechanism, wollastonite can capture and permanently store approximately 40% of its weight in CO₂. The precipitation of stable CaCO₃ in the form of calcite would bond together the sand and aggregate components of the concrete to form strong, rigid structures.

Wollastonite is a naturally occurring mineral that is supplied by NYCO Materials (www.nycomaterials.com). NYCO provides wollastonite in three grades of acicular powder;

- NYAD 100TM, with an average particle size of 55 µm;
- NYAD 400TM, with an average particle size of 9 µm, and;
- NYAD 5000TM, with an average particle size of 3.5 µm.

In North America, wollastonite is mined in New York State and in Mexico, and is produced in volumes of approximately 100,000 tonnes/yr.

If this entire volume of wollastonite was used as a cementitious material in CO₂-cured concrete, then approximately 25,000 tonnes of CO₂ per year would be stored (assuming that one tonne of wollastonite in concrete would react with 250 kg of CO₂).

DE-FE0004222, Task 2.0 (Business Evaluation) studied the US market for high-end countertop materials as a potential launch application for a wollastonite-based concrete product. This market, comprised of natural stone (eg. granite, marble, onyx), engineered stone and solid concrete, is scaled appropriately for the use of wollastonite as a cementitious material. High-end countertop applications in the US total 162 million ft² of surface area per year (equivalent to approximately 40 million ft³, or 3 million tonnes of concrete). In the long run, however, this demand would easily exceed the annual North American production.

The first stage of DE-FE0004222, corresponding to Technical Task 3, Subtasks 3.1 through 3.9, focused on defining the material and process requirements for a high-performance, wollastonite-based concrete.

The second stage of DE-FE0004222, corresponding to Subtasks 3.10 through 3.12 utilized a synthesized version of wollastonite, hereafter referred to as Solidia Cement, as a replacement for mineral wollastonite. Solidia Cement can be made in conventional cement making facilities utilizing the cement industry’s existing capital equipment, raw material supply chains, and distribution networks. This breakthrough eliminated the barrier to market penetration posed by mineral wollastonite production.

3.B. Subtasks 3.1 through 3.9

Quantify the wollastonite- CO_2 reaction. Recommend materials and process specifications for carbonated concrete manufacturing.

3.B.i Control of Mineral Particle Size

Wollastonite powder (NYAD 400) with a mean particle size of 9 μm was milled in a NETZSCH LabstarTM ball-milling machine. A 30 wt% suspension was prepared by dispersing 600 g of the NYAD 400 powder in 1400 ml DI water. The pH of suspension was adjusted to 12 using an appropriate amount of 2 M Na(OH) solution. Three grams of the surfactant Acumer 9400TM was also added to the suspension. The milling was performed under two different conditions as shown in **Table 1**.

Scanning Electron Microscopic (SEM) images of as-received and milled powder are shown in **Figure 1**. The as-received powder has a wide particle size distribution while the milled powder forms soft agglomerates (\sim 10-20 μm in diameter) after drying.

As the milling proceeds, the particle size continually decreases and consequently its specific surface area increases. A series of samples were collected at time points of 60, 120, 180, 240, and 290/270 min for SEM, BET, and light scattering particle-size measurements. **Figure 2(a-b)** depicts the effect of milling time on the mean particle size and specific surface area of milled powders.

Table 1. Milling conditions

	Condition 1	Condition 2
Mixer speed (rpm)	1050	1050
Pump speed (rpm)	400	400
Agitator speed (rpm)	2500	2500
Milling time (min)	300	300
Size of Zirconia ball (mm)	0.3	1.0

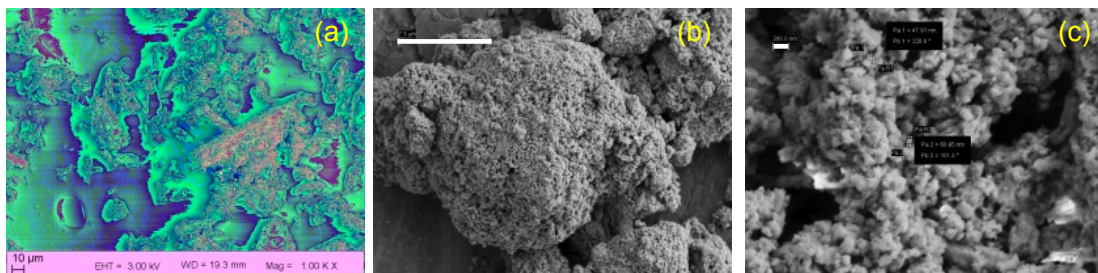


Figure 1. (a) As-received wollastonite (NYAD 400), (b) powder milled for almost 5 h with 1 mm zirconia balls, and (c) magnified image of (b). Scale bars for (b) and (c) are 7.5 μm and 200 nm, respectively

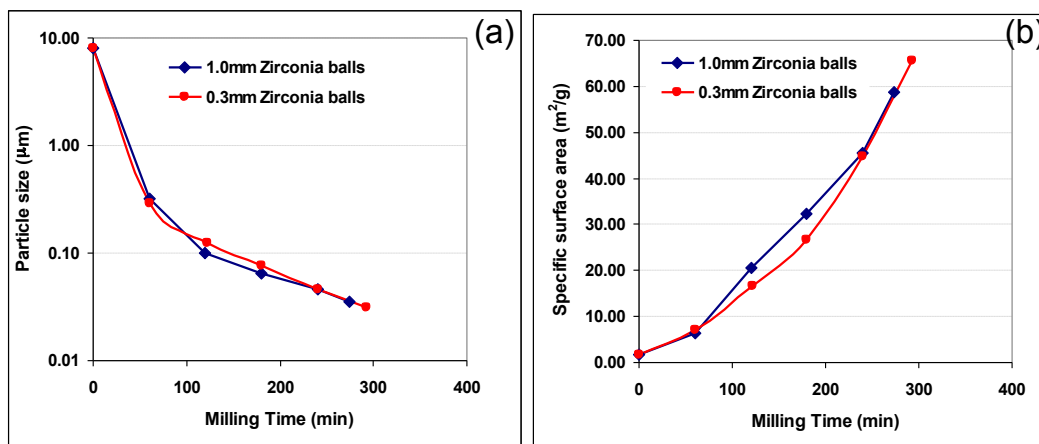


Figure 2. (a) Calculated mean particle size and (b) specific surface area of milled powder versus milling time

3.B.ii Methods to Measure Mineral Carbonation Rate and Yield

In-situ X-ray Diffraction:

A Brüker D8 Discover X-Ray Diffraction (XRD) unit, equipped with an in-situ reaction cell designed by Dr. Herbert Shaef at the Pacific Northwest National Laboratory, was utilized to determine the in-situ carbonation yield of NYAD 400 powder (**Figure 3**). The reaction was carried out at 60°C under 20 psi gauge pressure for 17 hours.

After placing appropriate amount of powder in the XRD sample holder, two drops of water were added onto the powder surface and 1 ml water was also introduced in the reactor chamber. The reactor cell was inserted in the cell holder and an XRD pattern acquired. The cell was then heated to 60°C. Once temperature was stabilized, the CO₂ gas was purged into the reactor cell and maintained at 20 psi gauge pressure. XRD patterns were collected over the 2θ angular range of 20–32° using the Göbel mirror for parallel beam geometry. The data acquisition was carried out every 10 min.

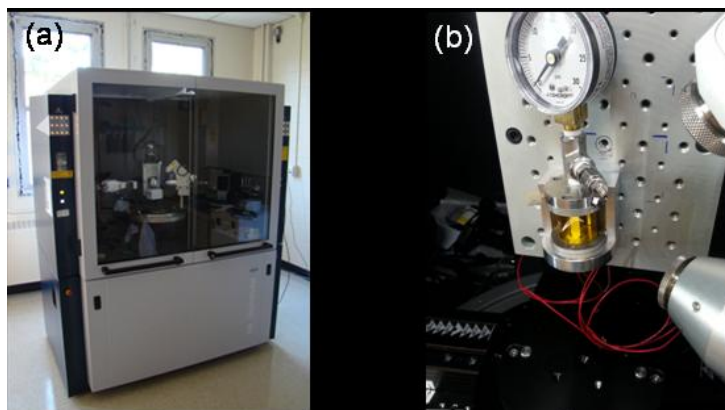


Figure 3. (a) The Brüker D8 Discover X-Ray Diffraction unit and (b) the in-situ reaction cell with Kapton window and heating stage

Three specific peak positions were used to track the crystalline phase evolution as the carbonation process progressed. **Figure 4a** depicts XRD patterns of NYAD 400 powder at 0, 8, and 17 hours of reaction. The peaks located at 26.15°, 29.31° and 29.81° belong to the aragonite, calcite and Wollastonite, respectively. As seen, the peak intensity of wollastonite decreased with increasing the reaction time while the peak intensity of calcite increased. **Figure 4b** depicts the intensity map of the

entire reaction process and clearly shows aragonite phase, which did not exist in the as-received powder, begins to form after 3 hours. These changes in peak intensities are presented in **Figure 4c**. The calcite yield, defined here as the ratio of CaCO_3 / wollastonite peak intensities, appears to have a linear relationship with the reaction time. The slope represents the reaction rate and its calculated value is equal to 3.3 % per hour.

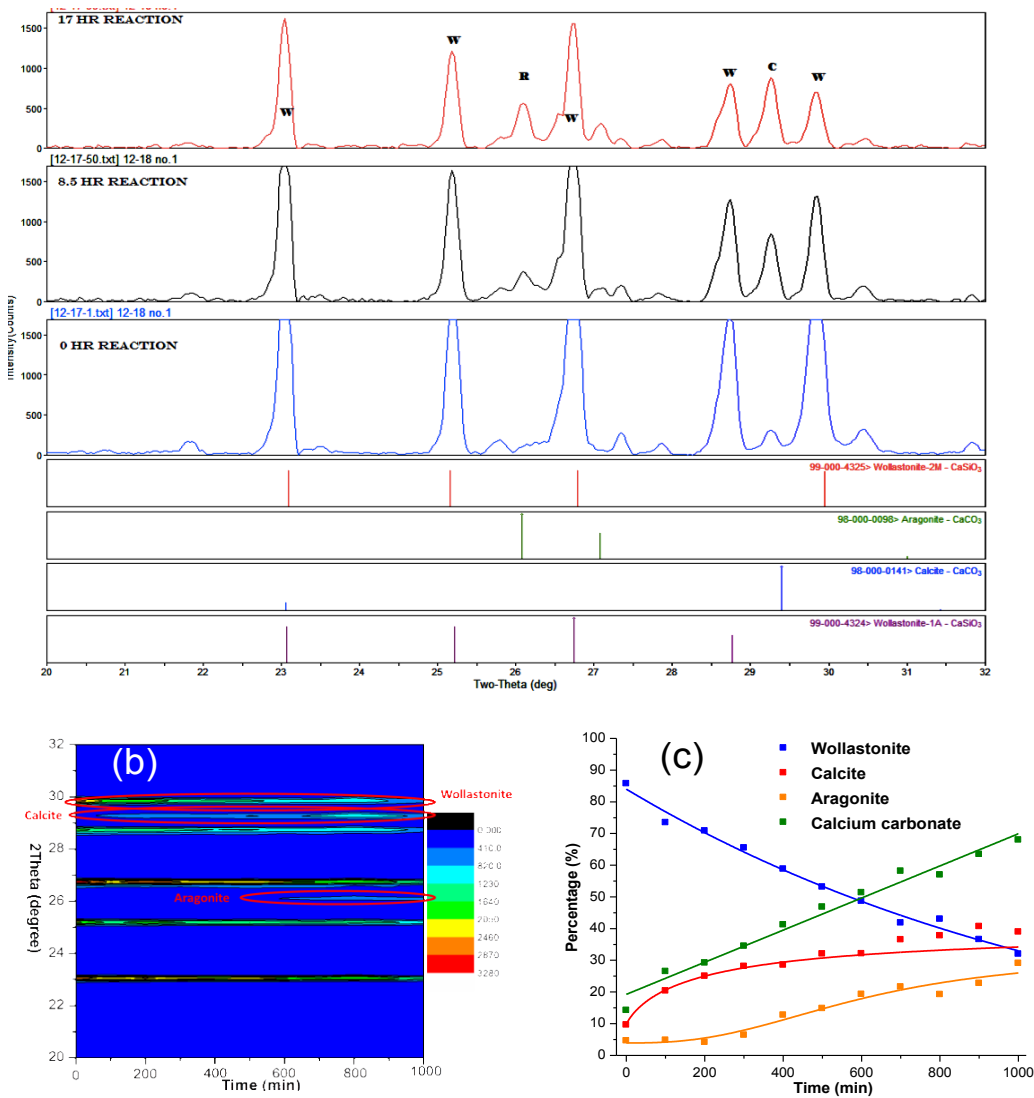


Figure 4. (a) XRD patterns of NYAD 400 powder at 0, 8, and 17 hours of reaction, (b) the intensity map of the entire reaction process (c) percentage of evolved phases versus reaction time

In-situ Fourier Transform Infrared Spectroscopy:

A Remspec Fourier Transform Infrared (FT-IR) spectrometer was used to measure the carbonation reaction kinetics of pressed pellets comprised of NYAD 5000 (**Figure 5a and b**). Samples were prepared by pressing a mixture of NYAD 5000 powder and 10 wt.% water into 25 mm diameter x 14 mm thick pellets having 50% theoretical density. De-ionized water was then dripped onto the pellets to saturate 50% of the pore volume. Reactions were performed at 90°C and 20 psig in a CO_2 gas atmosphere.

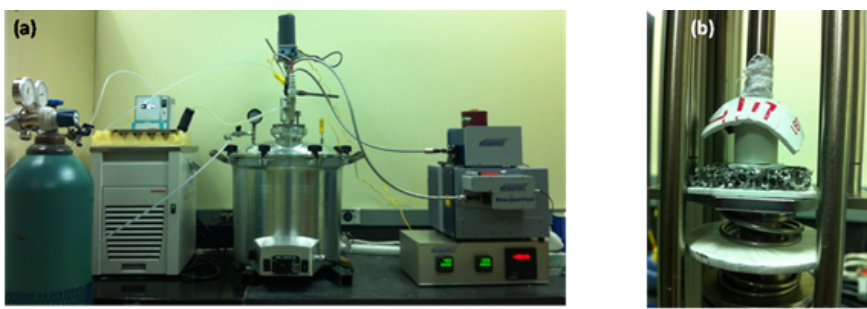


Figure 5. a) Remspec FTIR setup, b) sample with probe

Figure 6a displays a contour plot of the CO_2 reaction. As shown, any newly present chemical bond in the sample and its time of occurrence can be detected during the reaction run. **Figure 6b** depicts the IR spectra of reaction at various times. The IR bands of interest are: 1450 cm^{-1} representing carbonate species, 1070 cm^{-1} representing silica species, and 1015 cm^{-1} representing silicate species. Initial scans exhibited absorbance bands that were representative of wollastonite, while the final scans showed spectra with bands of mainly calcium carbonate and silica.

This observation can be clearly seen in the reaction trend lines graphed in **Figure 7a**. The peak of the absorbance band corresponding to calcium carbonate increased steadily and reached maximum after about 4 hours. Reaction was conducted for 330 min.

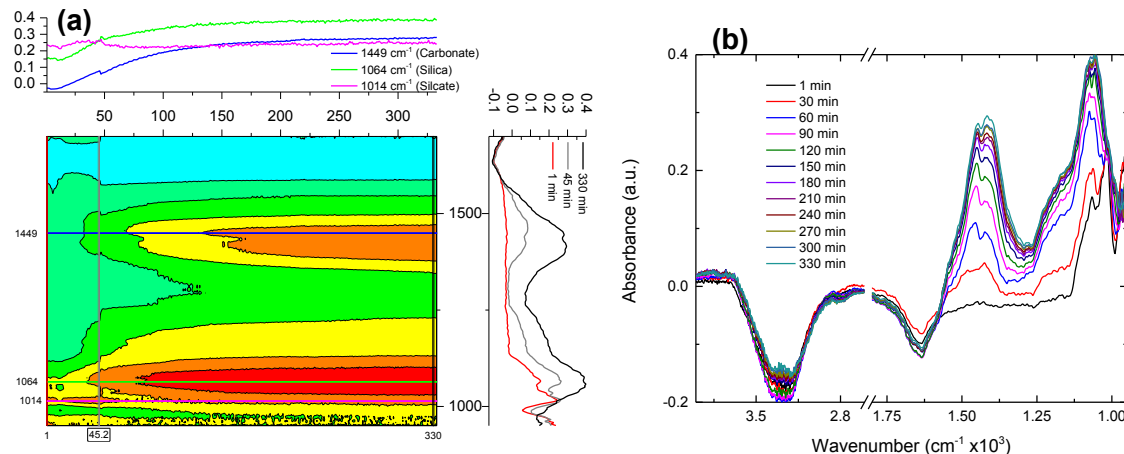


Figure 6. (a) Contour plot of in-situ FT-IR measurement of wollastonite during reaction with the IR spectra at different reaction times (right) and the absorbance trend lines for different wavenumbers (top). (b) the IR spectra of wollastonite during reaction

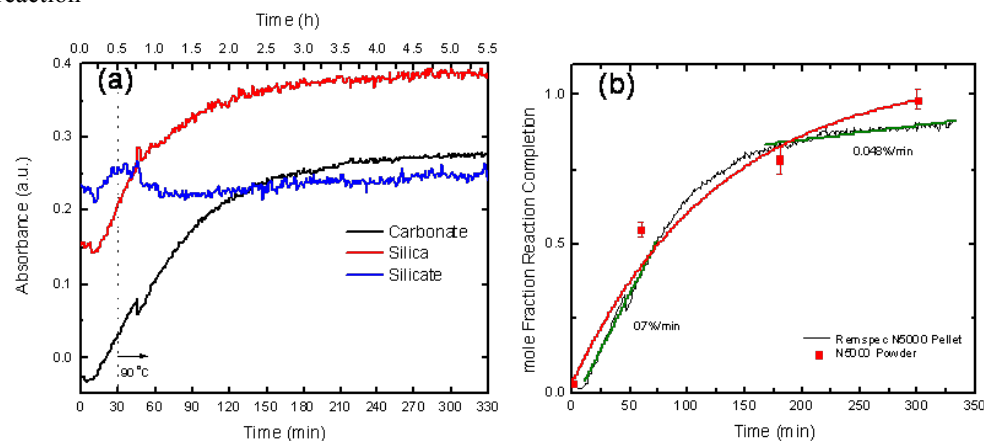


Figure 7. (a) Trend lines representing the peak intensities of carbonate, silica, and silicate over time, (b) the calculated mole fraction of carbonates from FTIR data and those obtained from the TGA analysis

Thermogravimetric Analysis:

The reacted pellets were also subjected to Thermogravimetric Analysis (TGA) in a TA Instruments Q5000 IR unit to analyze the carbonation degree of the sample. Weight loss was recorded between 25 and 1100°C at a heating rate of 10°C/min.

TGA plots and carbonation yields for reacted NYAD 5000 are illustrated in **Figure 8** and **Table 2** respectively. **Figure 7b** compares calcite mole fraction calculated from FT-IR data with those obtained from the TGA analysis. A good agreement between both methods was observed.

Figure 8: TGA of reacted NYAD 5000 powder

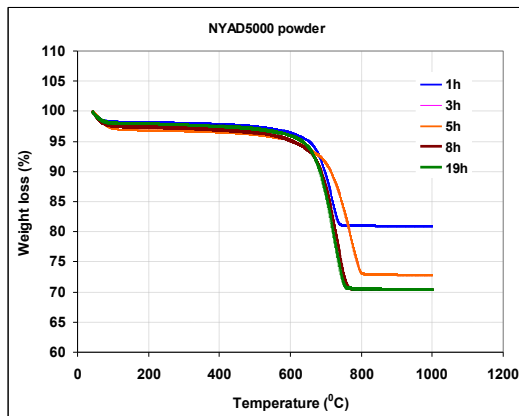


Table 2. TGA carbonation yields

Time	Reaction yield (%)		
	TGA	Calculated by eq. 4	Stan Dev
1	53.29	54.89	2.48
3	79.63	77.72	4.26
5	89.26	98.06	1.86
8	93.99	99.45	3.31
19	97.52	100	1.07

3.B.iii Mineral Carbonation Reaction Rate Dependence on Particle Size

The particle grinding techniques described in Section 1.2 and the carbonation reaction rate/yield measurement techniques described in Section 1.3 were used to compare various mineral wollastonite and synthetic wollastonite forms. **Table 3** list the materials studied, which included NYAD 5000, 400 and 100 in both “as-received” and “milled” forms, plus synthetic wollastonite. **Figure 9a** depicts the carbonation yield of these materials. In all cases, carbonation was carried out at 90°C and 20 psi gauge pressure.

Table 3. Specific surface area and mean particle size of various calcium silicates.

Sample/characteristics	SSA (m ² /g)	Mean PS (μm)	RXN rate (%/h) stage 1	RXN rate (%/h) stage 3
			stage 1	stage 3
NYAD100, ball milled (4 h)	0.7	47	12	1.8
Synthetic, as-received	1.7	18	8.7	1.4
NYAD400	1.8	9	22	1.07
NYAD5000	4.3	3.5	25	0
NYAD400, ball milled (24 h)	4	3	23.5	1.4
NYAD400, attrition milled (5 h)	99.8	0.02	22.5	0*

*heat treated at 650 °C for 4 hours.

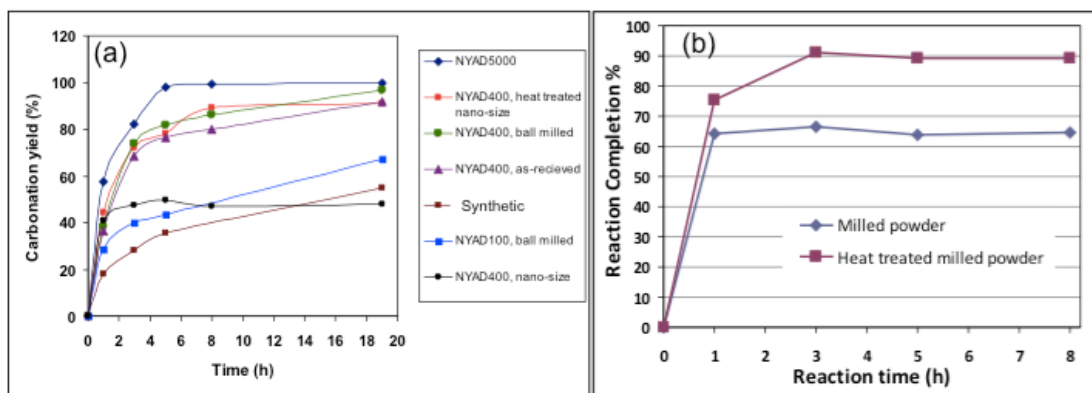


Figure 9. (a) Carbonation yields of (a) powders with various particle sizes and (b) nano-size milled NYAD 400 with and without heat treatment

The crystalline phase, specific surface area (SSA), and the mean particle size (PS) of calcium silicate have significant effects on the carbonation yield. The mineral wollastonite samples, which are entirely crystalline, generally react faster than the synthetic wollastonite, which is mostly amorphous. Large SSA and small PS result in higher carbonation rate and yield. These trends are evident in **Figure 10**.

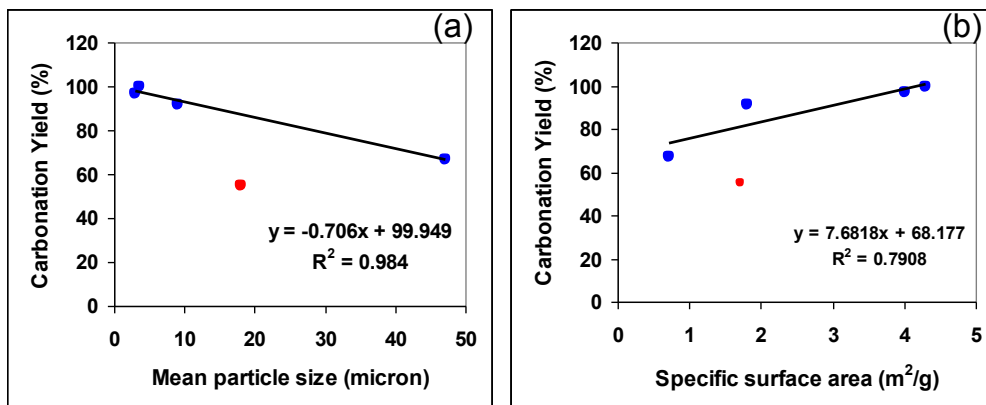


Figure 10. The effect of (a) mean particle size and (b) specific surface area of calcium silicate powders on carbonation yield. Powders were carbonated for 19 h at 90°C and 20 psi gauge pressure. The carbonation yield of synthetic wollastonite is shown by red dots

In addition, the reaction can be classified into 3 distinct stages of carbonation. In stage 1, carbonation occurs quickly and is followed by a transition period (stage 2). In the stage 3, the carbonation proceeds more slowly. The calculated carbonation rates (%/h) at stages 1 and 3 are also represented in **Table 3**.

As-received powders (NYADs 5000 & 400, and synthetic wollastonite) were also reacted for various times at 70 and 50°C under 20 psi gauge pressure. The results obtained are depicted in **Figures 11(a-b)**. The effect of temperature on carbonation yield is shown in **Figure 11c**. Reduction of reaction temperature did not have a significant effect on the yield of NYAD 5000 while it notably influenced the yield of NYAD 400. The carbonation yield of synthetic wollastonite remained unchanged by a 20 °C reduction in temperature (from 90 to 70°C). However, its yield sharply drops below 70°C.

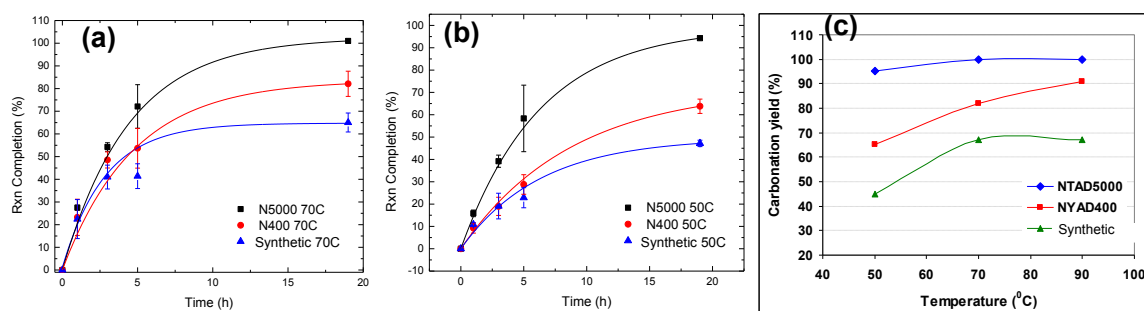


Figure 11. The carbonation yields of as-received mineral and synthetic wollastonites versus reaction time at (a) 70°C and (b) 50°C. (c) The effect of temperature on carbonation yields of these powders (19 h and 20 psig)

3.B.iv Mechanical Properties of Pressed and Carbonated Pellets

As-received mineral wollastonite (NYAD 100, 400 and 5000) and synthetic wollastonite were consolidated into disc-shaped pellets 25 mm diameter x 30 mm high. Approximately 25 g of powder was mixed with 10 g of water. The slurry was uni-axially pressed to the finished dimensions under a load of 120 MPa. At least five (5) pellets from each powder source were CO₂-reacted in an autoclave at 90°C for 19 hours under 20 psi gauge pressure. The reacted pellets were dried for 24 hours in a convection oven at 90°C. **Table 4** shows the starting powder characteristics plus the average green densities, reaction yields, and compressive strengths of carbonated pellets.

Table 4. Physical and mechanical properties of various wollastonite materials

Sample	Powder		Pressed pellets					
	SSA (m ² /g)	PS [d ₅₀] (μm)	Relative Density Green (%)	Reacted (%)	Rxn (%)	Std	Compressive Strength (MPa)	Std
NYAD100	0.6	55	0.76	78.83	11.33	5.39	30.09	21.29
Synthetic	1.7	18	0.63	72.66	39.68	4.97	100.64	61
NYAD400	1.8	9	0.64	76.21	50.11	2.2	177.97	20.15
NYAD400	1.8	9	0.64*	76.10*	50.14*	0.87*	175.24*	13.24*
NYAD5000	4.3	3.5	0.56	72.76	78.78	5.64	169.79	23.13

*Consolidated by slurry casting and cut into 25 × 25 × 50 mm test samples

As expected, the carbonation yield of pellets was directly and inversely proportional to the specific surface area and mean particle size of powder, respectively. Despite having the highest average green density, the NYAD 100 showed the lowest average values both for carbonation yield and compressive strength among all materials used. These findings were attributed to the smallest specific surface area and the largest average particle size of this powder. The NYAD 5000 pellets achieved the highest average carbonation yield while their average compressive strength was slightly lower than that of the NYAD 400 pellets. The former agreed well with the results obtained in Section 1.4, as NYAD 5000 powder was completely carbonated under similar reaction condition. The latter is most likely be due to the low average relative reacted density of the NYAD 400 specimens. The synthetic calcium silicate, a synthetic showed a lower carbonation yield and compressive strength when compared with NYAD 400 and NYAD 5000.

Demonstrating the highest compressive strength, NYAD 400 pre-forms (with both moderate relative density and carbonation yield) were selected to further investigate the effect of reaction temperature and pressure on the carbonation yield. Since consolidation technique had no influence on the physical and mechanical properties of pre-forms made from this powder (see **Table 4**), samples were prepared by the pressing method.

Figure 12 depicts the effect of temperature, reaction time and gauge pressure on the carbonation yield and compressive strength of NYAD 400 pellets. It shows the reaction degree and strength of samples reacted for 20 hours under 20 psi gauge pressure. The reaction temperature has a pronounced influence on improving both characteristics, especially between 20 and 50°C. A ~35% carbonation could give rise to pellets with ~150 MPa compressive strengths. A one-to-one correspondence appeared to be present between the carbonation yield and compressive strength. Further increase of reaction temperature slowly enhanced the degree of carbonation and compressive strength. In general, a non-linear relationship was observed between temperature/time and these characteristics.

The reaction completion versus time for samples reacted at 90°C and 20 psi gauge pressure is depicted in **Figure 12 (c-d)**. Both carbonation yield and compressive strength reached plateaus at 20 hours, increasing negligibly up to 70 hours.

The effect of CO₂ pressure on the carbonation yield of the NYAD 400 pellets was also studied. Pellets were carbonated for 20 hours at 90 °C, with gauge pressure ranging from 2 to 20 psi. **Figure 12 (e-f)** shows that the gauge pressure has only a slight effect on carbonation. This could be attributed to the fact that even at 2 psig, the effective CO₂ pressure under this reaction condition was 6.8 psi, which is quite enough to give rise to high carbonation yield and corresponding compressive strength.

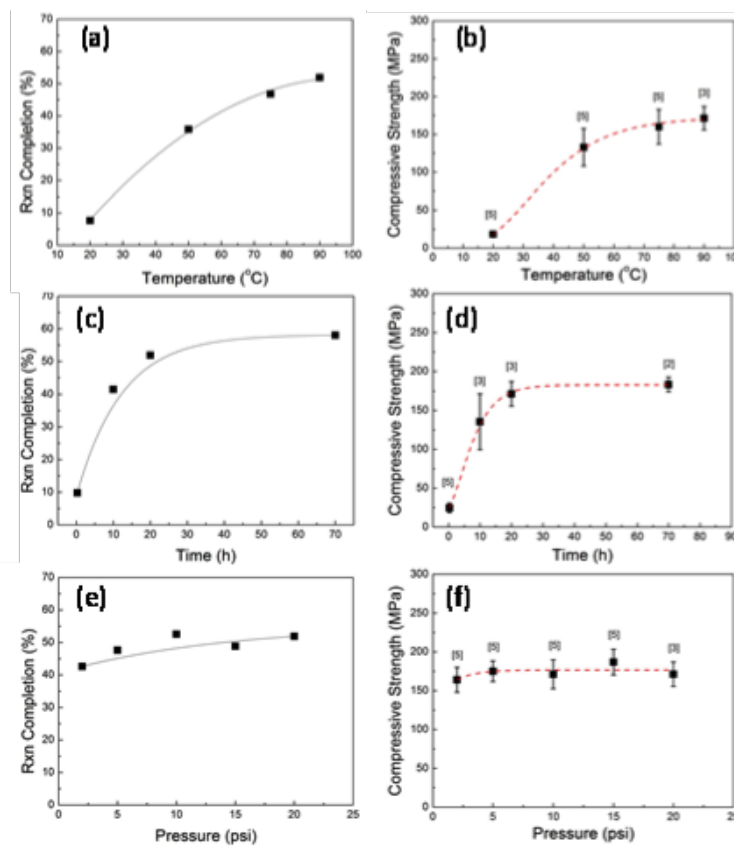


Figure 12. (a) Carbonation yield and (b) compressive strength of NYAD 400 pellet reacted under 20 psig versus temperature. (c) Carbonation yield and (d) compressive strength of NYAD 400 pellet reacted under 20 psig versus time. (e) Carbonation yield and (f) compressive strength of NYAD 400 pellets reacted for 19 h at 90°C versus pressure gauge

3.B.v Summary: Selection of a Raw Material Formulation & Carbonation Process for Making Building Panels

The studies described above provide practical guidelines for establishing both materials and carbonation process specifications for a wollastonite-based, concrete system.

Some of the primary observations governing material specifications are listed below:

- Mineral wollastonite, which exists in crystalline form, reacts with CO₂ both faster and more thoroughly than synthetic wollastonite, which exists in amorphous form:
- Fine, high surface area wollastonite particles (ex. NYAD 5000 with $d_{50} \sim 3.5 \mu\text{m}$), react significantly faster and more thoroughly than coarse, low surface area particles. This obviates the need to subject wollastonite to costly milling processes.
- Coarse wollastonite particles (ex. NYAD 100 with $d_{50} \sim 55 \mu\text{m}$) compact more efficiently than fine particles, leading to superior green densities in pressed and cast forms.
- High compressive strength, a key requirement in most concrete products, was observed in samples comprised of intermediate wollastonite particle size (ex. NYAD 400 with $d_{50} \sim 9 \mu\text{m}$) and intermediate green density. It should be noted that NYAD 400 has approximately the same mean particle size as Type 1 Portland cement.

From a process standpoint, several additional observations are noteworthy:

- Pressing, extrusion and casting appear to be viable processes for forming wollastonite-based concrete products.
- Carbonation reaction times of at least 20 h are required to reach peak compressive strengths. This time is consistent with the initial curing time for Portland cement-based concrete.
- Carbonation reaction temperatures of 70 to 90°C are required to reach high carbonation rates and yield. Carbonation rates and yield drop precipitously at reaction temperatures of 50°C and lower.
- CO₂ pressure during the carbonation reaction had little effect on carbonation rate or yield.

3.C. Subtasks 3.10 through 3.12

Develop Solidia Concrete curing processes for full-scale precast concrete parts, utilizing synthesized Solidia Cement as a replacement for mineral wollastonite.

3.c.i Subtask 3.10 (Revised) Investigate Water Distribution Changes During Drying

Introduction to Drying

Many industrial processes involve working with wet porous materials that must be dried. Most wet porous materials pass through a constant-rate drying period and a falling-rate drying period as water is removed and the material passes from a wet state to a dry state.

Figure 13a shows how the free moisture in a typical wet porous material decreases with time as it is heated at a constant drying temperature. **Figure 13b** shows the drying rate for this material as a function of its free moisture content.

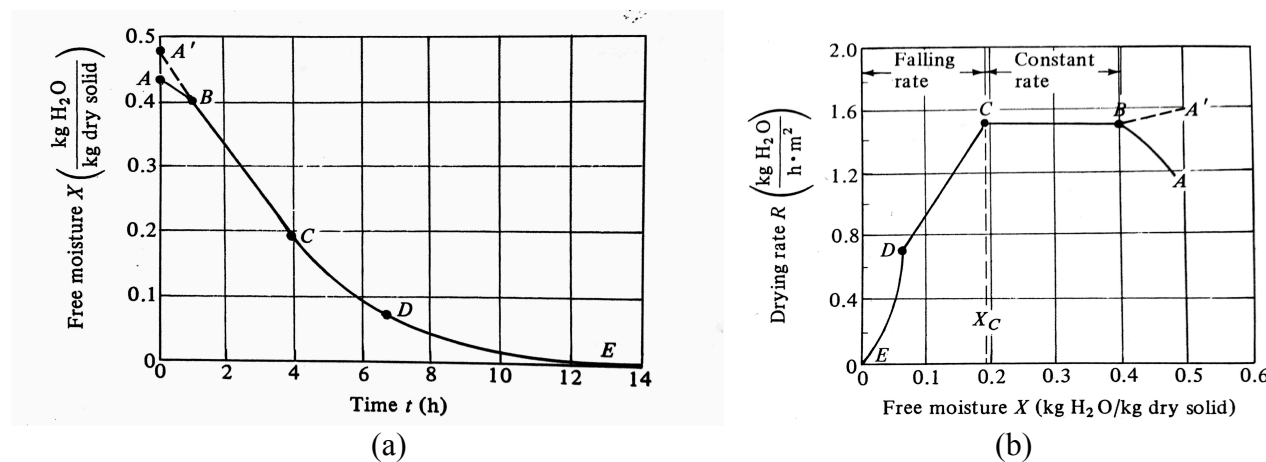


Figure 13. Typical drying curves for constant-rate and falling-rate periods

The period from point A to point B in Figure 1a is a transient-on period where the material is being heated or cooled to the initial drying temperature. The material reaches its initial drying temperature at point B where a constant-rate drying period starts and extends to point C. Moisture from the material's pores is continuously supplied to the material's outer surfaces by capillary forces during this period. The material's surfaces remain wet as water is removed from the material. The rate of drying is controlled by external mass and heat transfer between the exposed surfaces of the wet porous solid and the gas atmosphere with which it is in contact. The solid's surface temperature remains at the wet bulb temperature as water evaporates freely from these surfaces.

At point C in the drying process, capillary forces can no longer fully replenish the water that is being lost from the surface by evaporation. The moisture content of the porous material at point C is called the critical moisture content. From point C onward the drying rate decreases and the surface condition moves toward a completely dry state as water coverage of the surface diminishes. The period immediately after point C and extending to point D is known as the first falling-rate period of drying.

At point D in the drying process, water in the pores of the wet solid begins to recede from the exposed surface. The fraction of surface covered by water decreases with time. Water evaporation continues in the pores where the wet bulb temperature prevails. However, the temperature of the exposed surface rises toward the dry bulb temperature of the gas with which it is in contact.

The time period extending from point D to point E is called the second falling-rate period of drying. Water empties from the pore space in the solid during the second falling-rate period. The emptying process is complex and depends on the pore structure, pore sizes, and material composition. The position of point D, between points C and E in **Figure 13b**, is often not distinct. Also, the change from a partially wetted to completely dry condition at the surface can be so gradual that no sharp change is detectable.

Constant Rate Drying Period

As shown in **Figure 13b**, drying starts with the constant-rate drying period. To derive the equations for calculation of drying rate, we neglect heat transfer by radiation to the solid surface and also assume no heat transfer by conduction to the sample surface. Under these assumptions, the surface temperature is the wet bulb temperature T_w . The rate of convective heat transfer q from the gas at T to the surface of the solid at T_w is

$$R_c = \frac{q}{A\lambda_w} = \frac{h(T - T_w)}{\lambda_w} \quad (2)$$

R_c : drying rate, $\text{kg}/\text{m}^2 \cdot \text{s}$

q : rate of convective heat transfer, W

h : heat transfer coefficient, $\text{W}/\text{m}^2 \cdot \text{K}$

T : gas temperature, K

T_w : wet bulb temperature, K

A : exposed drying area, m^2

λ_w : latent heat of water at T_w , kJ/kg .

T_w is determined by the temperature and relative humidity and h is determined by the convective flow of gas to the sample surface. Thus, the drying rate is affected by temperature, relative humidity and gas flow.

Falling Rate Drying Period

After the constant-drying period is over, drying moves into the falling-rate period when water vapor diffusion from the sample controls the drying rate. Diffusion of water vapor occurs because there is a concentration difference between the depths of the solid and the surface. Using the concentration as X kg free moisture/ kg dry solid, Fick's second law for unsteady-state equation can be written as:

$$\frac{\partial X}{\partial t} = D_L \frac{\partial^2 X}{\partial L^2} \quad (3)$$

D_L : water diffusion coefficient in m^2/s

L : distance in the solid in units of meters.

The calculation method of D_L can be found in the reference (Geankoplis, C. J. *Transport Processes and Unit Operations*, 3rd edition, 1993, pages 552 - 556). In many cases, the average D_L is calculated from $X/X_c = 1$ to $X/X_c = 0.2$ where X_c is the kg free moisture/ kg dry solid at the beginning of the falling rate.

Solidia Concrete Drying

High Density Solidia Concrete

The high density Solidia Concrete drying example is the drying of a paver with a density of about 2,100 kg/m^3 . In this case the mix design was 16 wt.% Solidia Cement, 40 wt.% concrete sand, 20 wt.% sewer sand, and 24 wt.% $\frac{1}{4}$ " aggregate, with a small amount of admixture. Drying curves obtained by drying a paver sample in a 70°C air oven are shown in **Figure 14**.

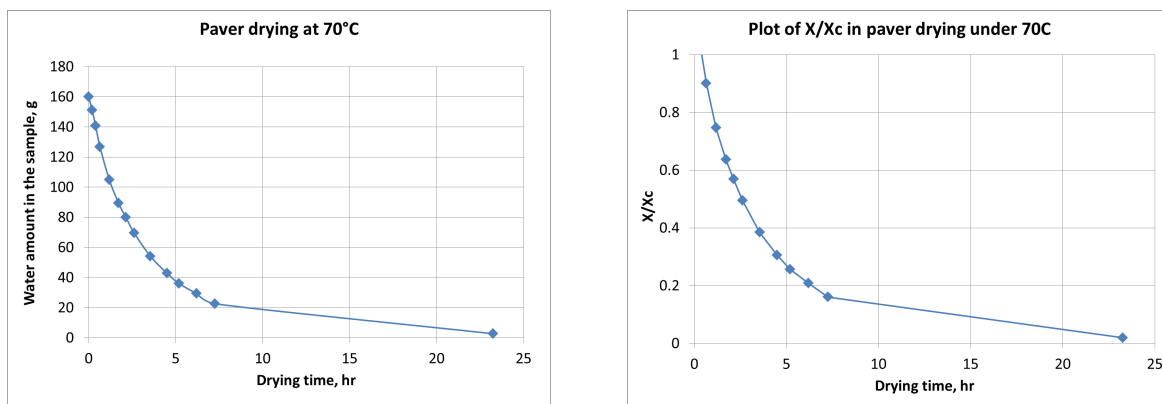


Figure 14. Paver drying curves

It took about 6.1 hours for the moisture content to fall from $X/X_c = 1$ (start of the falling rate) to $X/X_c = 0.2$. Calculated D_L (average water diffusivity from $X/X_c = 1$ to 0.2) = $2.3 \times 10^{-8} \text{ m}^2/\text{s}$ at 70°C .

Medium Density Solidia Concrete

A lightweight CMU block with an unreacted dry density of about 1600 kg/m^3 . The mix design was 15 wt.% Solidia Cement, 60 wt.% pumice, 20 wt.% sand, 5 wt.% 5mm aggregate, and a small amount of admixture. The total initial water amount in the lightweight block was about 15 wt.% of the dry-mix weight. Drying curves obtained by drying a CMU sample in a 50°C air oven are shown in **Figure 15**.

It took about 12 hours for the moisture content to fall from $X/X_c = 1$ (start of the falling rate) to $X/X_c = 0.2$. Calculated D_L (average water diffusivity from $X/X_c = 1$ to 0.2) = $2.0 \times 10^{-9} \text{ m}^2/\text{s}$ at 50°C .

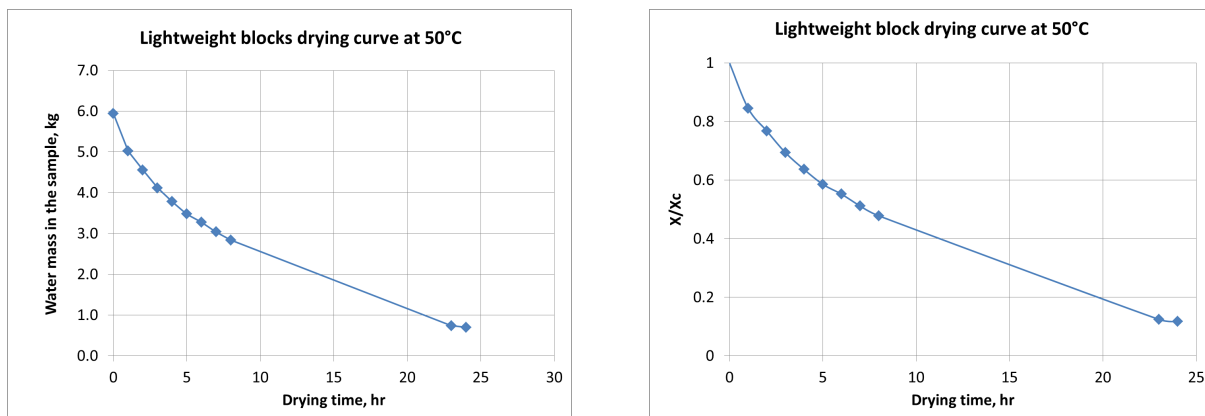


Figure 15. Drying curves of a lightweight block

Low Density Solidia Concrete

The low density Solidia concrete example is an aerated concrete block (6 inches by 6 inches by 10 inches) that underwent drying at 80°C . The mix design was 92 wt% Solidia Cement, 8 wt% lime (CaO), and a small amount of Al for aerating purposes. The initial water content in the aerated concrete mix was about 35 wt% of the dry-mix weight. After unreacted dry-density of the sample was about 700 kg/m^3 . The drying curves are shown in **Figure 16**.

Figure 16 reveals that the aerated sample had a 7-hour, constant-rate drying period. It took about 21 hours for the moisture content to fall from $X/X_c = 1$ (start of the falling rate) to $X/X_c = 0.2$. Calculated D_L (average water diffusivity from $X/X_c = 1$ to 0.2) = $4.3 \times 10^{-8} \text{ m}^2/\text{s}$ at 80°C .

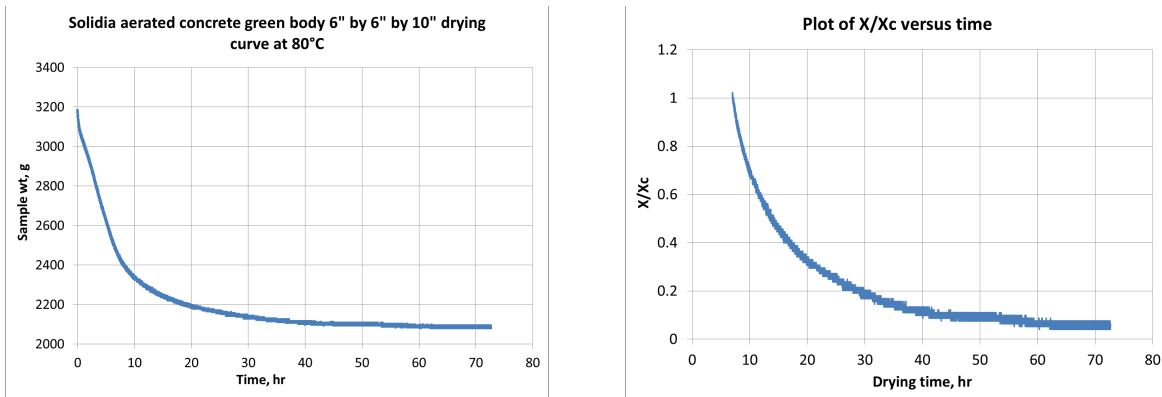


Figure 16. Aerated green sample drying curves

Drying Summary

Drying models for wet, porous materials were reviewed as the basis for understanding the drying behavior of Solidia Concrete. Drying curves were then obtained from various types of Solidia Concrete products, including high-, medium- and low-density samples. Each of the concrete forms studied show clearly demonstrated a defined constant-rate drying period and an internal-water-controlled falling-rate drying period.

Utilizing the drying models in conjunction with the actual drying curves enabled the calculation of the average water vapor diffusivity for each of these samples. This allowed the prediction of important CO₂-curing variables such as temperature, humidity and gas velocity. These predictions served as the basis for subsequent Subtasks 3.11 and 3.12.

3.C.ii Subtask 3.11 (New) Investigate Water Distribution Changes During Curing

In this subtask, a qualitative conceptual framework for describing the physical and chemical changes that take place in the Solidia Concrete curing process was developed. The end objectives were to understand the relationship of the drying and curing processes, and to build intuitive and quantitative pictures of the curing process.

Evidence for reaction fronts

The development of curing and drying fronts during the curing of Solidia Concrete is evident upon examination of product specimens from a wide range of interrupted curing runs as seen in **Figure 17**.

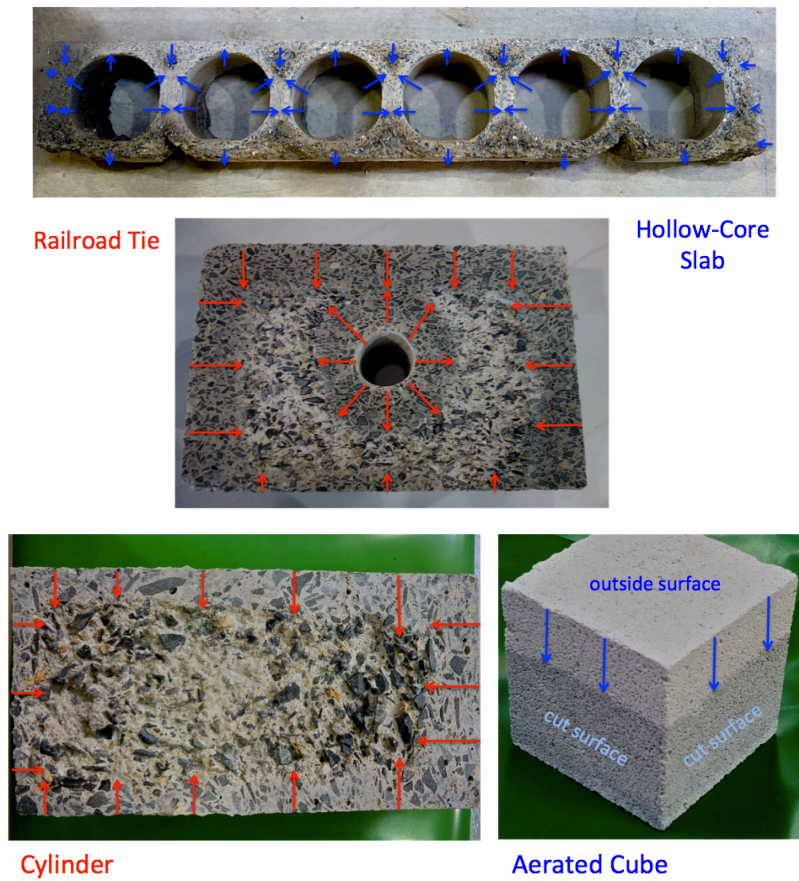


Figure 17. Pictures of front development in various types of Solidia Concrete product cross-sections
(Top) Hollow-core slab cross-section measuring 4 feet wide x 8 inches high. (Middle) Railroad Tie cross-section measuring 12 inches x 8 inches. (Bottom left) Cylinder cross-section, 4-inch diameter x 12 inches long. (Bottom right) 2-inch cube cut from a larger piece of aerated concrete

For both the hollow-core slab and the railroad tie, it appears that a drying/reaction front moved inward from the core surfaces and from the outside surfaces of the object. In the case of the cylinder the fronts progressed toward the cylinder's center from its outside surfaces. In each of these cases, frontal retreat from one surface was slower than frontal retreat from the remaining faces. Slow movement was associated with the face that was in contact with a supporting surface during the curing run. The support obstructed mass transport of water and CO₂ through the one face that was blocked. The front movement in the case of the aerated cube is seen to be along a single direction because the specimen was cut from a larger piece of concrete. Evidently, as shown by the color change, the reaction front in this case was planar.

Evidence for coupled drying and curing reaction fronts

The process of curing a Solidia Concrete hollow core slab involves flowing CO₂ gas around and through the slab. Heat is transferred into the slab from the gas through the slab's top and side surfaces as well as the surfaces that form the cores. The bed, upon which the slab has been extruded, is heated so that heat also flows into the slab through the slab's bottom surface. CO₂ and H₂O gases counter diffuse within the pore structure of the slab, which enables the chemical conversion of CaSiO₃ to CaCO₃ and SiO₂, which comprises the curing process.

A model four-channel hollow core slab measuring 4 ft by 2 ft by ½ ft was cast for this study. The as-cast slab comprised aggregate, sand, Solidia Cement and water. The slab was heated from the bottom surface using electrical heating pads. Bed temperature was ramped from 28C to 90C over two hours and maintained at 90C for the duration of each experiment. The heated slab was cured in preheated CO₂ gas. Thermocouples were embedded at various positions within the slab so that changes in temperature within the slab could be followed as a function of time during the curing process. The experimental set-up is illustrated in **Figure 18**.

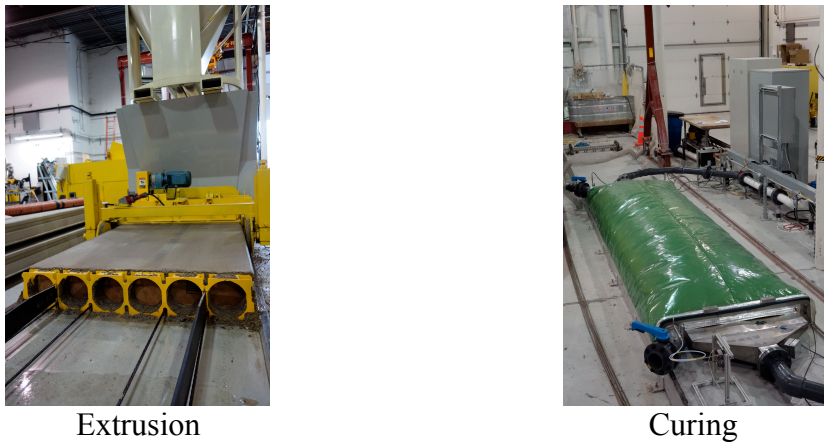


Figure 18. Solidia Concrete hollow-core slab test bed

A sequence of three experimental runs were completed using a single slab:

- **Run 1** was a normal curing run in which the slab was reacted with flowing CO₂ until it was completely dry. Thermocouple temperatures varied because of heating, drying (an endothermic process), and carbonation (an exothermic process).
- **Run 2** was a repeat of the first run using the dry hollow core slab produced in run 1. Thermocouple temperatures varied because of heating alone, since the slab was already dry and the absence of water precluded any further carbonation.
- **Run 3** was a repeat of run 2 except that the pores within the slab were first refilled with water and then air was used to dry the slab (instead of CO₂ gas as in a normal curing run). Thermocouple temperatures varied because of heating and drying.

Figure 19 shows the results of Run 1 for thermocouples embedded at three different levels within the bed, as well as at the interface between the bed and heating pads. **Figures 20 and 21** show the corresponding results for runs 2 and 3 measured by the same thermocouples as in run 1.

Heating dominates the thermocouple response at the bottom surface because the temperature of the bed is constrained (controlled) to be a constant temperature. The relative influence of drying and reacting, compared to heating, increases as the thermocouple distance from the bottom surface increases. Thus the blue curves in the figures contain the largest signals for the drying and reacting processes.

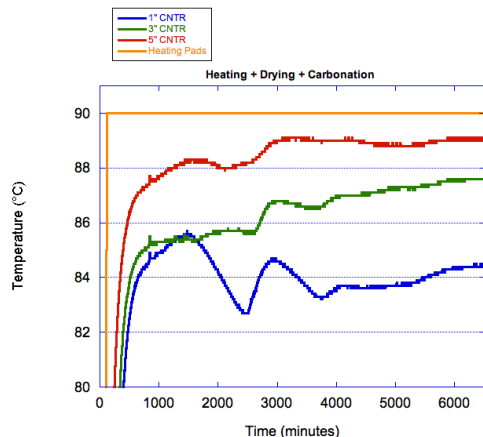


Figure 19. Thermocouple responses during the curing process

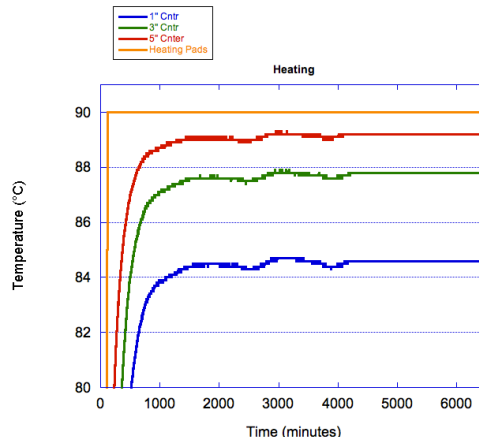


Figure 20. Thermocouple responses due to heating alone

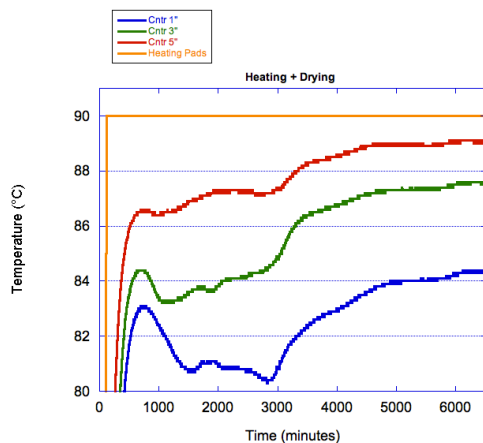


Figure 21. Thermocouple responses due only to heating and drying together

Subtraction of the blue curve for run 2 from the blue curve for run 3 shows the response of the thermocouple buried 1" below the top surface due to drying alone. Subtraction of the blue curve for run 3 from the blue curve for Run 1 shows the response of the thermocouple buried 1" below the top surface of the slab due to carbonation alone.

These temperature difference curves are shown in **Figure 22**.

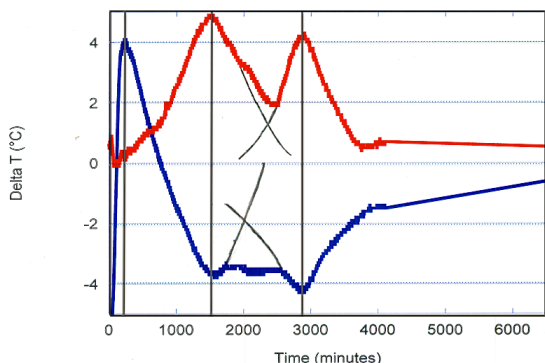


Figure 22. Endothermal effect of drying as function of time (blue) and exothermal effect of carbonation as a function of time (Red) during curing of Solidia Concrete

These experimental results suggest that the drying component of the curing process and the reaction (carbonation) component of the curing process are strongly coupled. A model emerges wherein the curing reaction starts from the (topological) outer surfaces of the object being cured and proceeds inward. Evaporation of water, followed by counter diffusion of CO_2 (inward) and H_2O (outward), sets up a drying front, which is more-or-less coincident with a reaction front. Within the frontal region we have the correct mix of CaSiO_3 , CO_2 and H_2O to support the curing reaction. Liquid water fills the pore structure on the inward side of the front where the curing reaction is starved for CO_2 , the availability of which for reaction is limited by slow liquid phase diffusion. Evaporated H_2O is rapidly being depleted from the reaction zone on the outward side of the front by diffusion and removal at the object's surface. Thus, the curing reaction is starved for liquid H_2O on the outward side of the front. The curing process ends when the various impinging fronts collide.

The appearance of a pair of drying peaks separated by about 20 hours (and a matching pair of reaction exotherms) in **Figure 22** suggests that two reaction fronts swept past the thermocouple probe during the experiment. This observation is consistent with the view that the curing slab had a bimodal pore distribution and that water empties faster from the larger pores than from the smaller pores.

Evidence for constant rate and falling rate curing-drying periods

The relative humidity during the curing process, shown in **Figure 23**, can be divided into three periods. In the first period, the band of relative humidity measurements remains relatively constant. In this period, water is evaporating from the surface of the hollow-core slab and the evaporated water is being replaced by water from the interior of the slab. Interior water is driven to the surface by capillary forces. The first period corresponds to the classical constant drying-rate portion of the drying curve for a porous solid.

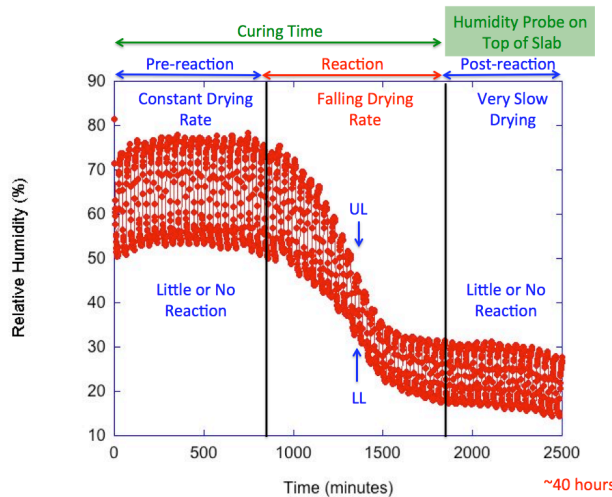


Figure 23. Time evolution of the relative humidity envelope during the curing of a hollow-core slab

In the second period, capillary forces can no longer supply enough water to the surface to replenish the water that is being lost by evaporation. A drying front establishes itself as water vapor begins its outward diffusion through the pore structure of the slab and CO_2 gas diffuses inward at the same time. A reaction front establishes itself and moves inward with the drying front. Ahead of the drying front the carbonation reaction does not have enough CO_2 . Behind the drying front the carbonation reaction does not have enough water. At the position of the reaction front CO_2 (g), CaSiO_3 (s) and H_2O (l) are present in sufficient concentration to support the curing reaction. The upper and lower limits of relative humidity fall as water is removed from the interior of the slab by diffusion and inwardly diffusing CO_2 is consumed by the curing reaction. The second period corresponds to the classical falling-drying-rate portion of the drying curve for a porous solid.

In the third period, relative humidity is essentially unchanging. Either reaction front impingement is complete or there is no longer sufficient water to further cure the slab. Further curing is impossible without adding more water to the slab.

Temperature measurements during the curing cycle confirm this analysis. A rise in the slab temperature is noted during the falling rate-drying period, which would correspond with the exothermic carbonation reaction.

Similar experiments were conducted on Solidia Concrete railroad ties and aerated concrete. These led to the same general conclusions. Specifically, the drying and curing reaction fronts are strongly coupled, and the simple drying process, and the coupled curing-drying process exhibit constant rate and falling rate drying characteristics.

3.C.iii Subtask 3.12 (New) Find the Optimum Curing Conditions for Sample Size, Geometry and Density

In Subtasks 3.10 and 3.11, water distributions during Solidia Concrete drying and curing were studied. In Subtask 3.12, this information is applied to the development of optimized Solidia Concrete curing processes.

In an existing concrete manufacturing environment, raw materials may vary from batch to batch (due to moisture and temperature), and multiple product mix designs and product geometries must be accommodated within a single curing environment. Yet, it is recognized that optimal curing parameters may change as products vary in density, composition, forming water content and dimension. In subtask 3.12, specific curing processes have been developed for pavers, concrete blocks, hollow core slabs and railroad ties.

Use of Computational Fluid Dynamics to determine uniformity of curing parameters

Computational Fluid Dynamics model for a paver curing chamber

As described above, it is crucial for the Solidia Concrete curing process to be reliable, repeatable, and economical. To meet this objective, computational fluid dynamic (CFD) models are used to understand and aid in the design of gas flow in large chambers. The goal is to obtain uniform humidity and temperature throughout large curing chambers during the curing process.

An ideal curing chamber design should achieve the following goals:

- Uniform drying of all the products in the chamber in a reasonable length of time;
- Ability to install the system within the limited space available;
- Low installation costs;
- Applicable to all chambers at the customer facility, and;
- Minimize energy use.

The model geometry was developed using the commercially available three-dimensional CAD and mesh generation software, GAMBIT V2.4.6. The computational domains generated for the model consisted of approximately 10.5 million tetrahedral, hexahedral, and polyhedral cells.

The CFD software package ANSYS-Fluent v14.5 was used to calculate the full-scale, three-dimensional, incompressible, turbulent flow throughout the chamber. A stochastic, two-equation realizable k-e model was used to simulate the turbulence. Detailed descriptions of the physical models employed in each of the Fluent modules are available from ANSYS-Fluent.

The overall size of the commercial curing chamber that was studied is in excess of 135,000 cubic feet. The model, and subsequent experimental confirmation, involved approximately 1/17 of the full chamber, or about 8000 cubic feet. The volume modeled represents a “unit cell” (which will be referred to as a “sliver”) of the full chamber. The content of the unit cell is replicated by translation to obtain the retrofit volume.

In the model chamber, the sliver has a capacity of 14 large trays of bullnose pavers. Each tray holds 42 pavers for a total of 588 pavers. The modeled volume is approximately 4-ft wide, 17-ft high and 6-ft deep. Dimensions of the pavers, trays, overall chamber, and sliver CFD model are given in **Table 5**.

Table 5. Parameters used in the CFD model

Geometry:	Units	Metric	Units	English
Curing Chamber Dimensions				
Length	(m)	21.946	(in)	864
Width	(m)	3.658	(in)	144
Height	(m)	5.182	(in)	204
Volume of Empty Chamber	(m ³)	415.918	(ft ³)	14688.0
Sliver Model Dimensions				
Length	(m)	1.212	(in)	48
Width	(m)	1.857	(in)	73
Height	(m)	5.182	(in)	204
Volume of Empty Chamber	(m ³)	11.656	(ft ³)	411.6
Sliver Volume Fraction	(%)	2.80%		
Tray Dimensions:				
Length	(m)	1.100	(in)	43.34
Width	(m)	1.400	(in)	55.16
Height	(m)	0.016	(in)	0.625
Volume of each Tray	(m ³)	0.024	(ft ³)	0.865
Block Dimensions:				
Length	(m)	0.305	(in)	12
Width	(m)	0.060	(in)	2.375
Height	(m)	0.152	(in)	6.000
Gap Between Blocks on Tray	(m)	0.013	(in)	0.500
Exposed Surface Area per Block	(m ²)	0.125	(in ²)	194
Volume of each Block	(m ³)	2.74E-03	(ft ³)	0.097
Blocks per Tray	(-)	42		
Trays per Level (Sliver)	(-)	1		
Number of Levels	(-)	14		
Number of Trays	(-)	14		
Number of Blocks	(-)	588		
Total Volume of Trays	(m ³)	0.343	(ft ³)	12.1
Total Volume of Blocks	(m ³)	1.608	(ft ³)	56.8
Packing Efficiency = (V_block + V_tray) / V_chamber	(%)	16.7%		

The model anticipated using 6-in x 12-in sheet metal ducts were used to feed gas to each level of the sliver. Gas was injected through two 7/8-in diameter holes in the duct for each level in the sliver. In the actual field installation, the ducts will be constructed using cruciform vanes inside the duct to ensure that the gas jet exhausts in the desired direction. The gas return duct was also a 6-in x 12-in sheet metal duct, but with a single 2-in diameter hole for extracting gas.

The model was tested with three different jet orientations. The first orientation was with the jets parallel to each other, and directed straight across the chamber. This resulted in reversed flow between the jets. In an effort to reduce the reversed flow, the jets were each angled outward at 15° from the duct axis. This resulted in reversed flow between the jets. Finally, the model was tested with the jets oriented at 7.5° from the duct axis, which resulted in reversed flow in both locations. In the end, the difference in surface conditions on the blocks with the different jet orientations was negligible. In fact, the straight jets provided the best conditions in many categories. These results are shown in **Figure 24**.

The final inlet and outlet duct sizing and hole positions resulted in a uniform temperature and humidity distribution within the chamber using realistic input gas conditions (80°C, 30% RH), as shown in **Figure 25**. It is notable that with a uniform withdrawal in the outlet duct, the gas near the top of the chamber (level 14) is slightly hotter and drier than the gas at the bottom of the chamber (level 1). This difference is small, but it suggests a single withdrawal point near the bottom of the chamber may improve performance.

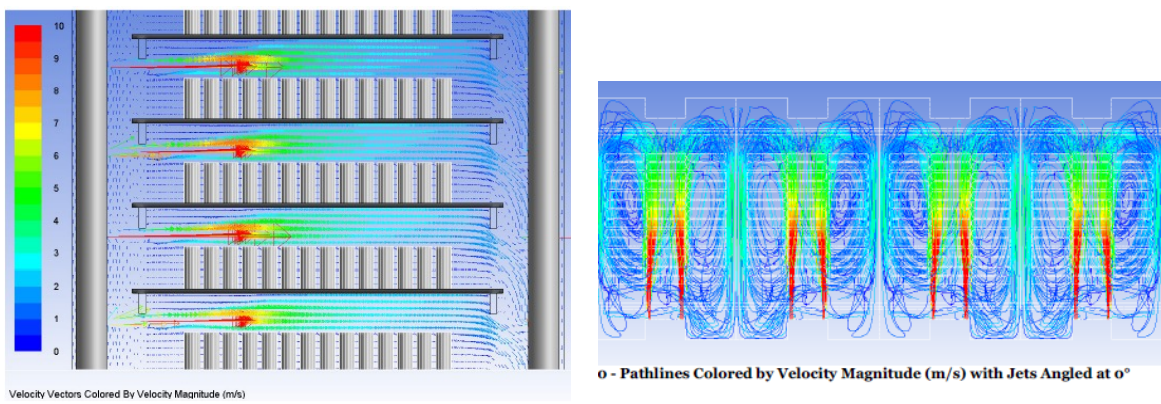


Figure 24. Side view (top) and top view (bottom) of gas flow pattern

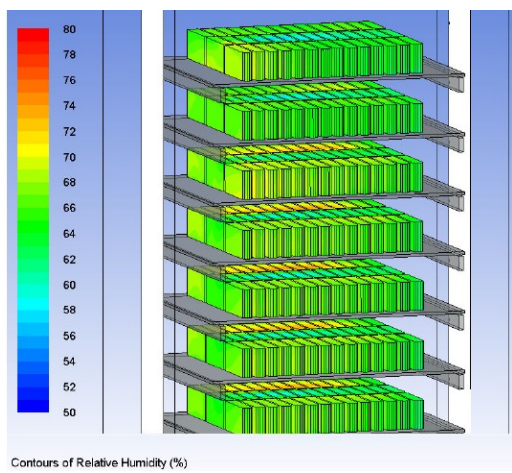


Figure 25. Relative humidity contours within the curing chamber

Experimental confirmation for paver curing

To evaluate the accuracy and usefulness of the CFD models, a partial physical replica of the computational model was constructed. This physical model had the same width and depth as the computational sliver model, but was shorter, having just 5 product shelves as opposed to 14 in the model. All other spacing and ducting was identical to that used in the model. **Figure 26** shows the frequency distribution of water vapor mole fraction at the surface of all of the products outputted by the CFD model at steady state. **Figure 27** shows the frequency distribution of water vapor mole fraction measured in the physical model.

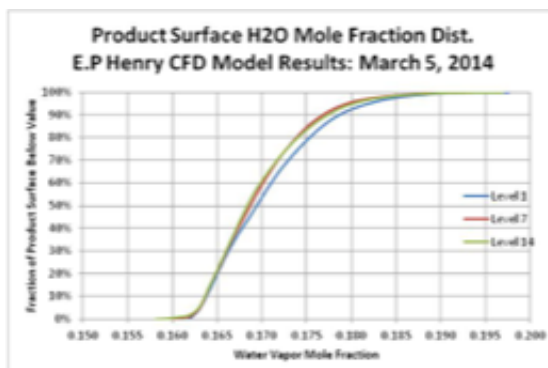


Figure 26. Model frequency distribution of water vapor mole fraction

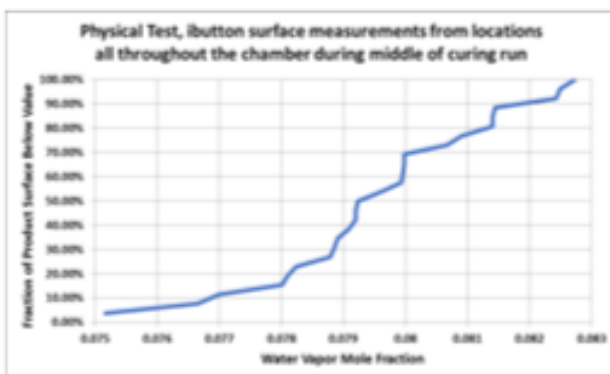


Figure 27. Measured frequency distribution of water vapor mole fraction

The physical model was operated under milder drying conditions (40 °C lower temperature, 10% higher relative humidity and 50% lower flow) than was used in the computational model for the sliver. Thus, the magnitudes of the measured mole fractions of water were smaller than the mole fractions calculated for the sliver (by about 50%). Interestingly, the measured range of the water distribution was narrower than the range calculated for the sliver (by about 33%), so that the uniformity of the humidity in the physical test was superior to the uniformity of humidity calculated for the sliver at more severe drying conditions.

Table 6 shows that the standard deviation for the water mole fraction obtained in the physical replica yields 2.25%, as compared to 3.53% for the CFD model.

Table 6. Width of frequency distribution of water vapor mole fraction

	Avg. Mol Fraction	Max	Min	Stdev % of Avg
CFD Model	0.170	0.197	0.158	3.53
Physical Replica (Run #397)	0.0796	0.0827	0.0752	2.25

Based on these findings, high drying uniformity and therefore high curing uniformity is expected throughout all of the products cured in the physical replica chamber. In fact, cured pavers in the physical mockup chamber were found to have very uniform amounts of residual water independent of their position in the chamber. It is therefore believed that using CFD models will facilitate the design of large chambers that yield repeatable, reliable and uniformly cured products.

Demonstration of uniform curing in other concrete product forms

Concrete Masonry Units

Figure 28 is a photograph of the Columbia press that is installed at Solidia Technologies and used to form pavers and concrete masonry units (CMUs). CMUs are also commonly known as concrete blocks.



Figure 28. Columbia block and paver press

CMUs are formed using vibratory compaction and require a certain amount of forming water, dependent on the mix, to form and evenly disperse Solidia Cement binder throughout the CMU. The required amount of water for forming the CMU (~5.0 to 5.5 weight %) is higher than the water requirement necessary to convert calcium silicate to calcium carbonate during CO₂-curing (~3.0 to 3.5 weight %). Thus, the removal of the excess water becomes a critical process requirement.

Pre-curing drying is the process of evenly removing the excess forming water from the product before the CO₂-curing takes place. The goal of pre-curing drying is to uniformly reduce the water content from the forming level to the ideal curing level. **Figure 29** is a photograph of CMUs that were unevenly dried under non-uniform drying conditions. The dark areas were dried to the target level of ~3.0 weight % water. The light areas were dried to water levels of 1.0 to 1.5 weight %. When CO₂-cured, these CMUs yielded a wide and unacceptable range of compressive strengths.



Figure 29. Unevenly dried Solidia Concrete CMUs

CFD models for curing chamber temperature and relative humidity were created to assist in developing a uniform environment for pre-curing drying. Nozzles and CO₂ flow rates were adjusted to create the additional turbulence required for a uniform relative humidity profile within the chamber. This result is illustrated in **Figure 30**. Uniformly dried CMUs, resulting from this process adjustment, are shown in **Figure 31**. These CMUs were all dried to the target water levels.

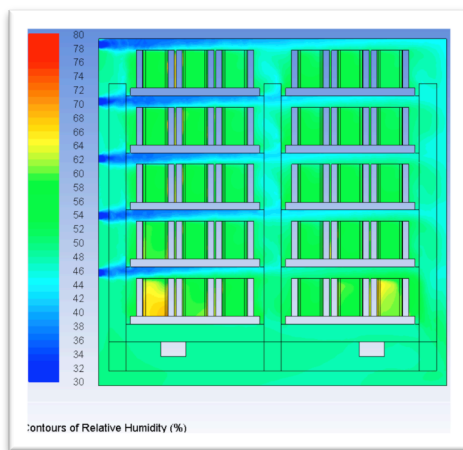


Figure 30. Contour plot of relative humidity throughout the chamber with modifications



Figure 31. Evenly dried Solidia Concrete CMUs

Railroad Ties

The unique geometry and size of a railroad tie (**Figure 32**) dictated the design of a specialized CO₂-curing chamber (**Figure 33**). The mass of a railroad tie is approximately 300 kg, compared to a 3 kg mass for a paver or a CMU. The curing chamber for the railroad tie provides for large CO₂ flow rates, necessary to remove the large amount of water present in the massive concrete piece, while maintaining a sealed environment. By employing the knowledge gained from the paver and CMU drying and curing experiments, full-size railroad ties were CO₂-cured to target hardness throughout the tie cross section and along the tie length.



Figure 32. Solidia railroad tie before (left) and after (right) CO₂-curing



Figure 33. Railroad tie loaded onto curing cart (left) and sealed prior to carbonation (right)

To form the Solidia Concrete railroad tie, a concrete mixture having low water content and zero-slump was poured into the tie mold and compacted using an internal vibrating needle. The railroad tie was formed around steel rods that were removed after forming to create internal ducts. The internal ducts contributed to the amount of exposed surface area of the concrete product, which maximized drying rate and CO₂ penetration, facilitating the curing process. In actual railroad tie manufacturing, these ducts are

subsequently used to house steel reinforcement after curing is complete, giving the finished tie the required tensile strength. This production process is known as post-tensioning.

The physical characteristics of the railroad tie, such as total surface area, mass of water content, and density, influence the choice of starting CO₂-curing parameters. However, the complexity of the railroad tie shape necessitated close monitoring of the process itself. Localized temperature, relative humidity, and flow rate, plus overall water removal was measured in real time. In this manner, the extent of drying, and hence, of CO₂-curing, could be determined. As illustrated in **Figure 34**, complete curing of the railroad tie could be achieved within 15 hours (900 minutes).

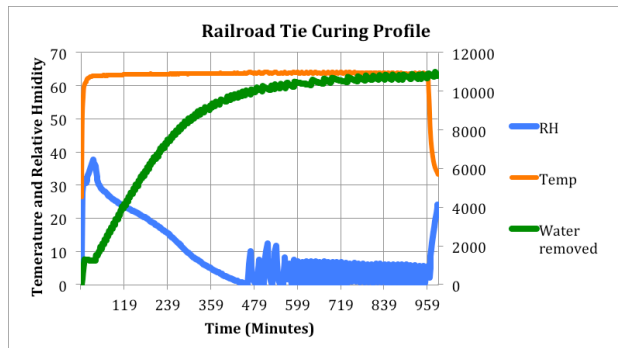


Figure 34. Optimized railroad tie curing profile

Hollow-Core Slab

As in the case of the railroad tie, the unique size and geometry of the hollow-core slab requires specialized CO₂-curing capabilities and monitoring. The curing set-up, described in Subtask 3.11, enables the CO₂ flow to be periodically reversed to prevent water buildup and condensation on one end of a 20 ft long, 5,000 kg concrete slab.

To optimize CO₂-curing of Solidia Concrete hollow-core slab, both the concrete mix design and the CO₂-curing process conditions were explored. Concrete mix design considerations were powerful. By reducing the forming water content of the concrete mix from 5.5 to 4.1 weight %, the constant drying rate period for the slab was reduced from 800 minutes to 60 minutes, as illustrated in **Figure 35**. Since Portland cement based slabs are typically cured within 20 hours (1,200 minutes) of extrusion, this reduction is critical for the practical use of Solidia Concrete in this application.

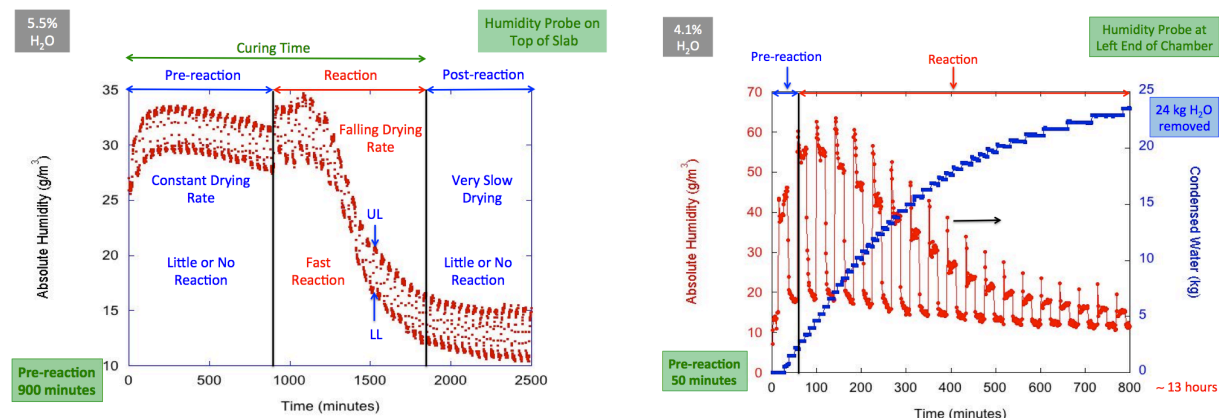


Figure 35: CO₂-curing humidity envelopes for hollow-core slab extruded with 5.5 (left) and 4.1 (right) weight % water in the concrete mix

Manipulations of the CO₂ circulation speed and the gas-flow reversal period were also useful in controlling the curing rate. **Figure 36** shows a base case for an 800 minute CO₂-curing exposure, wherein curing is performed with CO₂ circulation defined by a blower speed of 30 Hz (half speed) and a gas-flow reversal period of 60 minutes. As monitored by the absolute humidity and condensed water, full curing is achieved in about 10 hours.

Figure 37 shows a modified case where the time spent in the initial phases of falling-rate drying was extended. This was achieved by a) reducing the blower speed to 15 Hz (one-quarter speed) at the 100 minute mark, and then increasing the blower speed to 45 Hz (three-quarter speed) at the 200 minute mark, and; b) decreasing the gas-flow reversal period to 2 minutes at the 300 minute mark, and then increasing the gas-flow reversal period back to 60 minutes at the 450 minute mark. As monitored by the absolute humidity and condensed water, full curing time was reduced to about 8 hours.

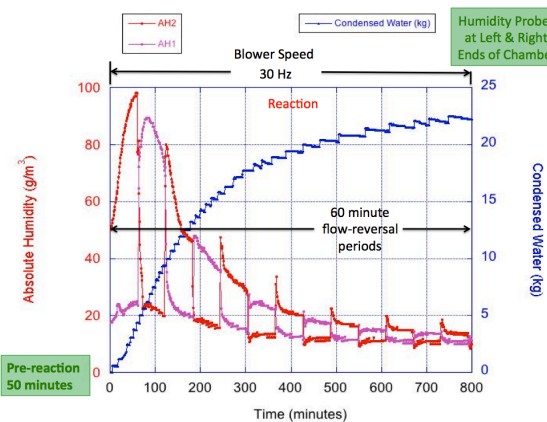


Figure 36. Base case for an 800 minute CO₂-curing exposure

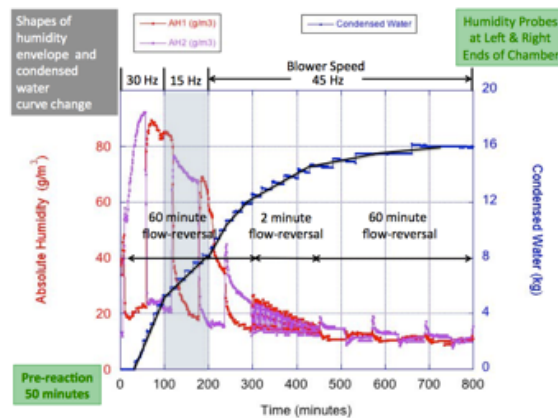


Figure 37. Influence of CO₂ circulation speed and the gas-flow reversal period on curing time

4. Demonstration of Commercial Application

4.A. Background

In March 2014, LafargeHolcim conducted a Solidia Cement production trial at the LafargeHolcim cement kiln in Whitehall, PA. Locally available limestone and sand, raw materials that are normally used for the manufacture of ordinary Portland cement were reacted using an unmodified cement production line to make approximately 7,000 tonnes of Solidia Cement clinker. The ratio of limestone to sand in the kiln feed and the temperature profile of the kiln were adjusted to produce an end-product with a Ca:Si ratio of 1:1.

The primary goal of the trial was to demonstrate the feasibility of Solidia Cement production in an existing commercial environment by reaching an acceptable cement quality and maintaining stable production for 3 days. This objective was achieved.

The cement production trial yielded valuable data for future production campaigns of Solidia Cement as well as a stock of cement that can be used during application commercialization trials as well as in research endeavors such as the DE-FE0004222 program. The average clinker chemistry and phase composition are shown in **Tables 7 and 8**. The average Ca:Si ratio for the cement was 1.06:1. The cement comprised four major phases: melilite, pseudowollastonite, amorphous phase and rankinite.

Table 7. Average elemental composition as measured by X-Ray Fluorescence (XRF)

Oxide	SiO ₂	CaO	Al ₂ O ₃	Fe ₂ O ₃	MgO	Na ₂ O	K ₂ O	SO ₃	TiO ₂	P ₂ O ₅	Mn ₂ O ₃
Mass (%)	43.2	42.76	6.00	2.47	2.03	0.14	1.06	1.00	0.27	0.23	0.07
	± 1.75	± 1.55	± 0.21	± 0.08	± 0.05	± 0.03	± 0.05	± 0.39	± 0.02	± 0.01	± 0.01

Table 8. Average clinker phase composition as measured by X-Ray Diffraction (XRD)

Phase	Mass %
Pseudowollastonite (CaSiO ₃)	22.3 ± 6.6
Wollastonite 2M (CaSiO ₃)	0.2 ± 0.1
Rankinite (Ca ₃ Si ₂ O ₇)	18.1 ± 4.1
Belite (Ca ₂ SiO ₄)	1.3 ± 1.8
Melilite ((Ca,Na) ₂ (Al,Mg,Fe ²⁺)[(Al,Si)SiO ₇])	30.5 ± 1.4
Bredigite (Ca ₇ Mg(SiO ₄) ₄)	0.3 ± 0.7
Quartz (SiO ₂)	2.8 ± 0.9
Cristobalite (SiO ₂)	1.9 ± 0.6
Tridymite (SiO ₂)	0.3 ± 0.2
Lime (CaO)	0.1 ± 0.0
Amorphous	22.2 ± 1.8

4.B. Subtasks 4.1 to 4.3

4.B.i Subtask 4.1 Demonstrate the basic performance of Solidia Cement produced at a commercial cement plant (LafargeHolcim, Whitehall, PA)

Milling and Powder Testing

Following the initial production of Solidia Cement clinker, 700 tonnes of clinker were slated for grinding. The material was milled using one of the existing finish-mill circuits in Whitehall. The milling circuit consisted of a two-compartment ball mill and a third generation separator. No gypsum was added to the material during milling. A commercially available cement grinding aid was added to the material feed at a level consistent with the level used during ordinary Portland cement production.

Solidia Cement powder was periodically sampled from particle separator output throughout the grinding operation. The particle size of this material was measured by laser scattering. Statistics from the particle size measurements are shown in **Table 9**. Particle size distributions were consistent throughout the milling process and comparable to those produced with Portland cement. Similarly, mortar flow tests performed according to ASTM C1437 were consistent and comparable to Portland cement mortars. The Solidia Cement mortars were prepared with cement and sand mixed in a 1:2.75 proportion and a water/cement ratio of 0.32.

Table 9. Particle statistics of Whitehall milled cement as determined by averaging particle size measurements throughout the grinding operation

Parameter	d10	d50	d90
Size (μm)	1.60	13.42	33.94
	± 0.10	± 0.69	± 2.04

Reactivity with CO₂

The rate of mass gain of the cement was measured by exposing a loosely packed powder bed to humid CO₂ at 30°C, 60°C, and 90°C. The Solidia Cement produced at Whitehall (referred to as “SC-W2 03” in the following experiments) was measured in parallel with samples of mineral wollastonite (CaSiO₃), rankinite (Ca₃Si₂O₇), and belite (Ca₂SiO₄). The results are normalized to the specific surface area of each material as measured by nitrogen adsorption (BET). The specific surface area of each sample is listed in **Table 10**. The normalized mass gain from 1 – 72 hours for each sample compared in **Figure 38**. The normalized mass gains of the sample cements show the reaction of the Whitehall cement surface is consistent with that observed for pure mineral wollastonite at 60°C and 90°C, and exceeds that of mineral wollastonite at 30°C.

Table 20. Specific surface area measurements of materials subjected to carbonation testing

Material	CaSiO ₃	Ca ₃ Si ₂ O ₇	Ca ₂ SiO ₄	SC-W2-03
SSA (m ² /g)	1.82	1.09	0.55	1.20

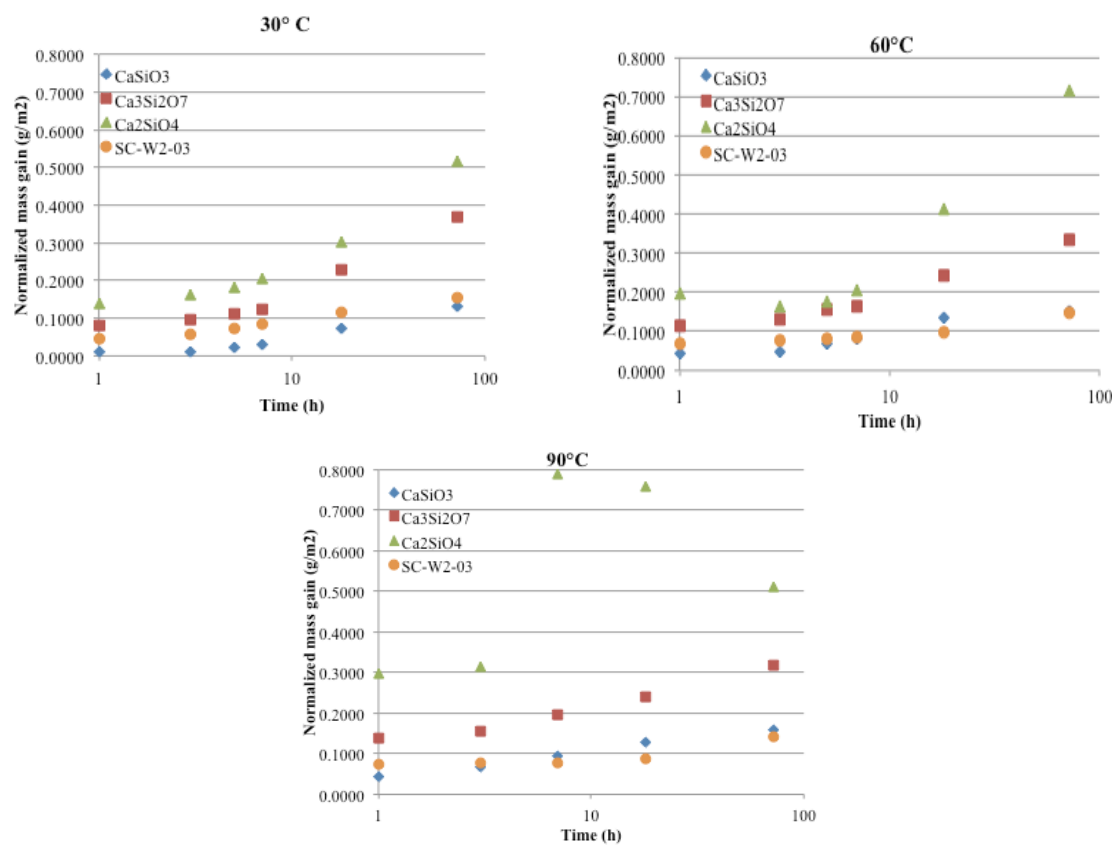


Figure 38. Normalized mass gain of Whitehall cement and synthetic carbonatable phases carbonated at 30°C, 60°C and 90°C

Concrete and Mortar Testing

A Whitehall cement mortar, described in **Table 11**, was evaluated according to ASTM C109. The W/C ratio of the mortar (0.28) was lower than that typically used for Portland cement mortars to allow for sufficient green strength for demolding of the samples. A water-reducing admixture was employed to achieve this W/C ratio. The specimens were demolded and cured at 60°C in a >99% CO₂ atmosphere with controlled humidity. The results of this test, along with reacted sample properties, are shown in **Table 12**.

Table 11. Composition of experimental mortar

Component	Cement	C109 Sand	Water	Water reducing admixture
Quantity	500g	1375g	140g	3.5 ml

Table 12. Results of the mortar cube evaluation

Compressive strength	Relative mass gain	Reacted density
8538 ± 269 psi	11.2%	2.11 g/cc

Concrete mixtures were prepared using the mixture proportion provided in **Table 13** with a targeted strength of 8,000 psi. As with the mortar, a water-reducing admixture was employed. The prepared concrete was cast into 4 inch x 8 inch cylinders and reacted at 60°C in a >99% CO₂ atmosphere with controlled humidity. Following the curing process, the concrete specimens were tested for compressive strength in accordance with ASTM C39. The compressive strength results and reacted sample properties are shown in **Table 14**.

Table 13. Experimental concrete mixture proportions

Cement	18%
Sand	31%
1/4" Aggregate	26%
3/8" Aggregate	25%
W/C Ratio	0.29
Water reducing admixture	7ml/kg cement

Table 14. Results of the mortar cube evaluation

Compressive strength	Relative mass gain	Reacted density
8183 ± 499 psi	12.3%	2.44 g/cc

The Whitehall cement achieved good performance in a mortar system and achieved the desired strength in the tested concrete system. The reactivity and performance of the cement in mortar and concrete systems indicate that this material can be used for products such as pavers and CMUs.

Summary

Solidia Cement produced in a commercial cement kiln was reacted with CO₂ in a high humidity environment. The mass gain of the cement during this reaction was measured to quantify the effectiveness of the carbonation reaction at various temperatures. The reaction was compared to samples of phase pure, carbonatable calcium silicates and normalized by the specific surface area of the cement. Analysis of this data indicates that the kiln produced cement shows a rate of mass gain per unit surface area consistent with a phase-pure carbonatable calcium silicate with similar bulk chemistry (mineral wollastonite with a molar CaO:SiO₂ ratio of 1:1) . This result indicates that the kiln-produced cement should have performance comparable to that of previously used carbonatable calcium silicates.

4.B.ii Subtask 4.2 Demonstrate the utility of Solidia Cement and initiate its commercialization in precast operations and applications

Phase 1 Precast Concrete Trials

The purpose of a Phase 1 trial is to successfully mix, form, and cure selected precast products made of Solidia Concrete. In each case, a concrete partner's mixing, forming and related process equipment was used in the partner's manufacturing facility to form concrete objects for curing. Product curing was conducted at the partner's manufacturing facility in a portable curing chamber supplied and operated by Solidia Technologies. The products produced during the trial were tested in accordance with both ASTM and the partner's local testing specifications. The objectives of the trial were tailored to suit the desired product or value items that the precast concrete partner wanted to evaluate.

Three trials were carried out at potential customer sites between January 1, 2015 and March 31, 2015. The first trial involved making concrete masonry units (CMUs or cement blocks); the second trial involved making two distinct types of roof tiles; and the third trial involved making hard-face pavers of several geometries and retaining wall blocks.

Partner ID and Selection

Solidia Technologies has developed three tiers of applications for commercialization based on regulatory hurdles, market acceptance time, and product geometries. Solidia's focus for the scope of this program will be on precast concrete products that fall in first two tiers outlined below.

Tier 1 applications include products that have low to no regulatory barriers (allowing for immediate market entry) and product geometries that Solidia Technologies has CO₂-cured in-house. These products include pavers, concrete masonry units (CMU's), roof tiles, and AAC (aerated concrete).

Tier 2 applications are products that have more stringent regulator barriers (typically light-duty structural concrete applications), and market entry times of a year or longer. These applications can vary in geometries based on customer application, but are generally much larger and more complex than the Tier 1 applications. These applications include hollow core slabs, architectural cladding, railroad ties, and concrete pipes.

Tier 3 products have the most stringent regulatory barriers (heavy duty structural and civil applications), and tend to be very large products. These applications include cast-in-place applications, bridge components, and large structural precast objects.

Solidia Technologies is engaging and partnering with industry-leading precast manufacturers who are focused on innovation, efficiency, and sustainability. These industry leaders can cover large geographies, and have multiple plant locations. This aids in the commercialization process, and gives multiple venues and applications. These industry partners produce products and practice processes to which CO₂-curing technology can add the most value.

Solidia Technologies is also partnering with LafargeHolcim, the world's largest cement manufacturer, to make Solidia Cement. LafargeHolcim also manufactures precast concrete products around the world. Solidia Technologies will be using LafargeHolcim's large marketing and sales force to help identify customers who fit the targeted selection criteria for participating in its trial and commercialization processes.

Codes

As it progresses towards full commercialization, Solidia Technologies has developed a strategy for gaining acceptance for cement and CO₂-cured concrete products in building codes and standards. In this context,

Solidia Technologies has been working with ASTM to integrate the new technology into its code structure. The primary area of focus has been ASTM C-01 (Committee for Cements). This committee steers all current codes related to cement, which are referenced in the majority of the generic and product-specific concrete standards.

Solidia Technologies has been gathering data, both in-house and through its research partners, which can be used to integrate Solidia Cement and Solidia Concrete into the relevant codes and standards. Solidia Technologies presented this research and data to the ASTM C01 executive committee at the 2015 ASTM annual meeting in New Orleans.

A crucial, upcoming decision will determine if Solidia Cement and Solidia Concrete can be added to existing specifications, or if new specifications will be required. Solidia Technologies will be working with the members of the ASTM community to decide which pathway will have the fastest time frame for implementation, and the greatest chance for acceptance by the cement and concrete communities.

Once Solidia Cement finds a place in a cement specification, focus will shift to changing existing concrete standards to reference the new cement specification. The timeline in **Table 15** outlines the remaining strategy for Solidia to gain acceptance for ASTM codes.

Table 15. Timeline for moving forward on ASTM codes

Action	Status
ASTM C01 executive committee	Complete
Debrief individual committee members	Complete
ASTM C01 staff consultation	Complete
Submit suggested “language” to C01 exec	June, 2016
Ballot Committee scopes language change	August, 2016
Defend language at ASTM meeting	December, 2016

Phase 1 Trial Summaries

Concrete Masonry Unit Trial

Solidia Technologies performed a Phase 1 demonstration trial to successfully produce normal weight CMUs (concrete masonry units) that met both strength ($\geq 2,250$ psi) and density (125 lb/ft³) specifications using Solidia Cement and CMU Manufacturer #1 forming and mixing equipment. During the trial, the Solidia Technologies team was able to modify the partner’s baseline mix design to produce CMUs that met the required specifications using Solidia Cement. The trial was successful in satisfying all the deliverables agreed upon by both parties.

Out of the eight batches cured, four contained CMUs that exceeded the ASTM C90 specification (2,000 psi) and three contained CMUs that met the customer strength specification (2,250 psi). Modifications to the mix design yielded a denser CMU with a reduction in the water required for the mix. The CMUs produced at CMU Manufacturer #1 are shown in **Figure 39**.



Figure 39. Normal weight CMUs on a curing rack

Roof Tile Trial

Solidia Technologies performed a Phase 1 demonstration trial to successfully produce flat and angled roof tiles (image at left) using Solidia Cement and the forming and mixing equipment at Roof Tile Manufacturer #1. The objectives of the trial did not include mix design optimization or curing condition optimization because the trial was carried out at a soon-to-be-closed site, which was still available for the trial. Commercial implementation of roof tiles will be at another facility.

Since roof tile extrusion was not possible at Solidia Technologies, in-house curing runs were impossible prior to this trial. Thus, the trial was performed without the benefit of prior experience. Nonetheless, production of extruded roof tiles with Solidia Cement was successfully demonstrated. The cured roof tiles met the partner's flexural strength specification according to ASTM C 293 (ballast pavers) and ASTM C 67 (angled roof tiles) after a 12-hour CO₂-cure. Pigment compatibility with Solidia Cement was also demonstrated.

Roof tiles produced at Roof Tile Manufacturer #1 are shown in **Figure 40**.



Figure 40. Flat roof tile in two colors

Hard Face Pavers and Retaining Wall Block Trial

Solidia Technologies performed a Phase 1 demonstration trial to successfully form and CO₂-cure hard face pavers and segmented retaining wall blocks at Paver and Block Manufacturer #1.

Hard face pavers produced with Solidia Cement and CO₂-cured for 16 hours surpassed the ASTM C936 specifications for compressive strength and freeze-thaw resistance. It was also determined that optimizing the mix design to reduce the amount of fine aggregate content in the paver could further increase compressive strength. Due to limited time, mix design optimization to bring down the cement content was not possible during the trial. The pavers also met Paver and Block Manufacturer #1's the aesthetic requirements for color. CO₂ sequestration was 15-18 wt. % of cement content. (i.e. Every 100 lb of cement consumed between 15 and 18 lb of CO₂).

Segmented wall sections were produced with Solidia Cement for the first time during the trial. The blocks were successfully cured and split (in post-production processing) after a 20-hour cure time. The

products were sectioned and testing according to ASTM C1372 specifications. The segmented retaining wall blocks met ASTM compressive strength requirement of 3000 psi.

A hard face paver and segmented retaining wall blocks produced at Paver and Block Manufacturer #1 are shown in **Figure 41**.



Figure 41. Hardface paver (left) and retaining wall blocks (right)

4.B.iii Subtask 4.3 Develop, optimize and implement curing processes required for cost effective and scalable manufacturing of Solidia Concrete for target precast concrete manufacturers

General Description of Phase 3 Technology Implementation

Solidia Technologies has developed novel CO₂-curing processes and is in the beginning stages of implementing these processes at commercial precast concrete facilities. Phase 1 technology implementation trials, discussed in Subtask 4.2, served to verify the ability to incorporate Solidia Cement and CO₂-curing processes with the products, processes, and equipment at a prospective customer's precast concrete facility. In addition to this verification, the compatibility of the CO₂-curing process with the customer's site is evaluated. Areas where this process can add value to a concrete manufacturer's products are explored and documented during Phase 1 trials.

Phase 3 implementations are designed to follow Phase 1 trials at specific precast concrete manufacturers. These implementations involve converting a single curing station to allow for production of a Solidia Cement-based product (*typical precast facilitates will have between 10 and 20 curing stations*). Phase 1 results, as well as the concrete manufacturer's willingness to adopt the technology, are considered when choosing a site for Phase 3 technology implementation.

After a site has been chosen for Phase 3 scale-up, Solidia Technologies will develop a model for incorporating CO₂-curing into the concrete manufacturer's curing chamber. Equipment will be specified based on modeling results, and a method for sealing the chamber to minimize CO₂ gas leaks will be engineered. After equipment installation is complete and the system is sealed, the Phase 3 commissioning process will begin.

Phase 1 trials were conducted at several facilities as described in Subtask 4.2. These facilities were evaluated for their potential to continue to the Phase 3 level. The following sections outlines specific details of work completed in the lead-up to and execution of the Phase 3 implementation.

Identification of Value-Added Attributes of Solidia Concrete

A detailed list of the potential value adding attributes of Solidia Concrete and Solidia Cement are laid out in **Tables 16 and 17** below.

Table 16 describes the general benefits associated with the adoption of Solidia Cement and Solidia Concrete technology. The benefits have been divided into product, process and sustainability categories to indicate the broad impact that Solidia's CO₂-curing technology can have on a manufacture's existing process. This table shows that the non-hydraulic nature of Solidia Cement has an added advantage, not just for the sustainability side, but also for the concrete product and the concrete manufacturing process. These latter categories offer significant opportunity to reduce manufacturing costs, reduce inventory costs, and improve field performance.

Table 17 includes the potential value proposition that Solidia and LafargeHolcim have identified when the technology is adopted for specific applications. The potential value proposition for each application has been determined through data collected from prior pilot trials at customer locations in the US. The value potential has not yet been validated on larger, production scale implementation, but once larger scale trials are run, these items will be validated. Each of the value proposition attributes have been identified in the left hand column of **Table 17**, and the specific product to which the attribute pertains is marked with an 'X'.

Table 16. Benefit summary of Solidia Concrete

Solidia Concrete™			
Benefit Summary			
	Product	Process	Sustainability
Cures w/ CO₂ (not H₂O)	<ul style="list-style-type: none"> No Ca(OH)₂ = improved durability No calcium hydroxide based efflorescence 	<ul style="list-style-type: none"> Ability to recycle fresh concrete waste. Non-hydraulic cement = faster clean-up times = increased production time Increased production flexibility 	<ul style="list-style-type: none"> ~3% of final products mass is permanently stored recycled CO₂ CO₂ converted to stable calcium carbonate Process water can be recycled, it is not chemically consumed
28-day strength in 24 hrs	<ul style="list-style-type: none"> Improved quality control 	<ul style="list-style-type: none"> Potential for improved inventory management, ready-to-ship production 	<ul style="list-style-type: none"> No added water during curing, steam curing not required
Additional	<ul style="list-style-type: none"> Similar mix designs Same aggregates Light cement color 	<ul style="list-style-type: none"> Same mixing / forming Minimal process modifications 	<ul style="list-style-type: none"> Local raw materials Potential carbon credit

Table 17. Potential value-adding attributes of Solidia's Cement and Concrete Technologies

VALUE PROPOSITION ATTRIBUTES PRECAST CUSTOMER MATERIAL SAVINGS OR PRODUCT IMPROVEMENTS	Normal and Lightweight Block	Architectural Block	Paver Products	Hollow Core	Architectural PreCast Panels	Roof Tiles
High Early Strength	X	X	X	X	X	X
Better Durability Properties	X	X	X	X	X	X
No Primary Efflorescence		X	X		X	X
Lighter Colour		X	X		X	X
Better Pigmentation		X	X		X	X
Cement Content Reduction	X	X	X	X	X	X
Admixture Reduction / Elimination	X	X	X	X	X	X
Less Concrete Waste	X	X	X	X	X	X
Curing Energy Savings						
Water Savings	X	X	X	X	X	X
Alternate Production Materials	X	X	X	X	X	X
Lower pH (No ASR; Potentially More Corrosive Environment for Rebar)	X	X	X	X	X	X
Shorten Production Cycle Time	X	X	X	X	X	X
Potential For Just-In-Time Production	X	X	X	X	X	X
Improved Inventory Mgmt. / Cash Flow	X	X	X	X	X	X
Faster Clean-Up	X	X	X	X	X	X
Streamline Post-Curing Processes		X	X			X
Smaller Curing Area / Racks / Boards	X	X	X			X
Extended Production Season		X	X	X	X	X
Reduced Equipment Maintenance	X	X	X	X	X	X

Capital Investment

The adoption of CO₂-curing at a precast concrete manufacturing facility will require a certain level of capital investment. The Solidia Technologies approach to this challenge attempts to minimize this investment. The bulk of the concrete manufacturer's processing equipment, including raw materials storage and conveyance, concrete mixing, concrete forming, and concrete product handling, will remain unchanged after conversion to CO₂-curing. The capital investment necessary to enable CO₂-curing is concentrated at the concrete curing station. Here, the capital investment can be divided into two distinct sections;

- The gas conditioning system, which manages the temperature, humidity and CO₂ concentration within the curing chamber, and;
- Mechanical modifications to the existing curing station.

The specific components of the gas conditioning system and modifications to the curing chamber are described in detail in this Section. It is projected that the conversion of an entire standard concrete paver and/or block manufacturing facility in this manner will require a capital investment of approximately \$1,500,000 (U.S.)

Manufacturing Costs

Table 18 presents a pro forma income statement ("pro forma") for a target concrete paver producer ("producer") located in the northeast section of the United States. The pro forma was prepared collaboratively between Solidia Technologies and the producer, and represents full conversion of one plant to CO₂-curing technology. It compares the current operation of the plant using Portland cement (PC) and water/steam-curing to the projected operation of the plant using Solidia Cement (SC) and CO₂-curing.

The first line of the pro forma, revenue, shows no gain from the producer's incumbent Portland cement system to the Solidia Cement system. This is believed to be a conservative assumption. It does not, for example, take into account premiums the producer can charge for green, sustainable products, nor does it account for overall increases in revenue resulting from potential market share gain.

Table 18. Pro forma Income Statement for Concrete Paver Manufacturer Converting to Solidia Technologies (000's)

	PC	SC	Value Add
Revenue	\$22,034	\$22,034	\$0
Cost of Goods Sold	\$19,418	\$18,775	\$643
Gross Margin	\$2,616	\$3,259	\$643
%	12%	15%	
SG&A	\$1,322	\$1,322	\$0
EBITDA	\$1,294	\$1,937	\$643
%	6%	9%	3%
Depreciation/Cost of Equipment	\$780	\$930	\$150
EBIT	\$514	\$1,007	\$493
%	2%	5%	3%
Interest	\$755	\$509	\$247
EBT	\$(241)	\$499	\$740
Tax rate	35%	35%	
Net Profit	\$(157)	\$324	\$481
%	-1%	1%	2%

The most significant impact of Solidia Technologies' CO₂-curing approach on a producer's business is reflected in a meaningful reduction in the cost of goods sold ("COGS"). Select product and process enhancements, as described in **Table 18**, produce a \$643,000 reduction in COGS. From a product enhancement perspective, COGS savings are realized in a reduction in certain admixtures required to

achieve certain mechanical and chemical properties, reductions in color pigments, reductions in costs associated with in-field efflorescence management, and the reduction in white cement usage due in part to Solidia Cement's light color. From a process enhancement perspective, COGS savings are realized in faster equipment clean-up, less process material waste, and reductions in both work-in-process and finished goods inventories. These projected enhancements reflect the field experience described and documented in Subtask 4.2.

The Solidia Cement system delivers a 25% gross margin increase over the incumbent Portland cement system. The pro forma assumes no change in selling, general, and administrative (SG&A) costs. Comparatively, the Solidia Cement system delivers a 50% increase in earnings before interest, taxes, depreciation, and amortization (EBITDA).

Producers should expect an increase in depreciation due to capital costs associated with the installation of new CO₂ gas handling equipment and curing chamber retrofit, in this case, an increase of \$150,000, effectively improving earnings before interest and taxes (EBIT) by 96%. The pro forma holds tax rates constant for both systems resulting in an increase in net profit of \$481,000.

An important factor to mention is that the pro forma assumes no value for any carbon tax savings. Solidia Technologies believes favorable economics related to forthcoming carbon tax programs will add substantial value to its value positioning.

Finally, project return estimates include a calculated net present value of \$2,687,000, a payback period of 3.3 years, and an internal rate of return of 44%.

Table 19 illustrates the specific value (plus or minus) associated with the unique attributes of Solidia Concrete properties and processes.

Table 19. Key System Cost Comparisons Per Ton of Cement

	PC	SC
Base Cost of Cement per Ton	\$97.08	\$112.06
Additional Materials/Savings		
Less cement required- Solidia more potent		(\$0.28)
PC higher pigment, SC lighter color requires less	\$0.06	
PC higher cost waste aggregate, SC less waste	\$0.28	
PC uses more admixtures, SC eliminates efflo ad mix	\$3.95	
PC miscellaneous ingredients eliminated		(\$0.22)
PC has high efflorescence claims, SC mitigates claims	\$26.44	
SC offers possibility of increased production capacity		(\$0.00)
PC higher scrap rates (pre-cure), SC does not harden and can be recycled	\$4.41	
PC has higher clean up costs, SC does not harden	\$11.02	
Reduced secondary process costs, SC can be done in line	\$8.81	
Processing advantages reduce SC system overhead costs		(\$4.19)
PC has higher waste (post-cure) than SC	\$17.63	
Capital cost for CO ₂ curing, added cost for SC System		\$41.42
CO ₂ tank rental, maintenance compliance for SC system		\$1.17
PC has higher inventory carrying costs vs. SC	\$9.87	
Premium price to customer for SC		(\$0.00)
Carbon tax savings for SC system		(\$0.00)
Total system costs	179.55	\$149.95
Overall SC System Advantage Compared to PC System		\$29.60

Rational Behind Selection of Paver and Block Manufacturer #2

The selection of Paver and Block Manufacturer #2 for Solidia Technologies' first commercial curing chamber conversation was an important decision based on several criteria including geographic location, product line offering, addressed market, ownership support, and finally, a culture supportive of innovation.

Proximity to the Solidia Technologies plant in New Jersey, as well as positioning in an important downstream commercial market, were both important factors in geographic site selection. Close proximity to the Solidia Technologies plant enabled convenient access for plant engineers and technicians to visit the customer site with the frequency and flexibility necessary to undertake a pilot conversation. Additionally, Paver and Block Manufacturer #2 is situated within 200 miles of one of the largest residential and commercial construction markets in the United States, offering attractive access to distribution channels and quality end-use prospects.

Paver and Block Manufacturer #2's broad product offering in the landscape/hardscape segment aligned nicely with Solidia Technologies' stated desire to commercialize pavers and blocks. Further, their reach into both residential and commercial end-use markets helps ensure broad application possibilities for the CO₂-curing technology. Finally, Paver and Block Manufacturer #2's executive leadership demonstrated active involvement in all phases of the commercialization project, supported fully by an innovative culture both willing and able to execute production and subsequent market entry strategies.

Paver and Block Manufacturer #2 operates production plants in five locations in New Jersey and Pennsylvania. The largest of the plants is located in New Jersey and consumes approximately 25,000 tonnes of cement per year. The combined cement consumption of all of the production plants under the umbrella of Paver and Block Manufacturer #2 is approximately 57,000 tonnes.

The New Jersey plant is split into two production areas: one for the production of concrete blocks and the other for the production of pavers. Each of these production lines includes concrete mixing capability, a dedicated vibro-casting machine, and a bank of curing chambers. Solidia Technologies and Paver and Block Manufacturer #2 have focused on the production of pavers during the Phase 3 implementation.

Description of the Concrete Curing System

Paver and Block Manufacturer #2 cures pavers in tall, narrow chambers, shown in **Figure 42**. Racks of uncured pavers are robotically loaded into the chambers. After the racks have been loaded, roll-down doors are closed before beginning the curing cycle.

The chamber selected for the Phase 3 conversion is the end chamber on the paver product line. This bay was selected on the basis of its location. As an end chamber, Solidia Technologies was able to convert the enclosure to a CO₂-curing system with minimum impact on the remainder of Paver and Block Manufacturer #2's production. It will also allow access to the location through a large overhead door located in the back of the building.

The chamber is approximately 5 ft wide (double bay is 10ft wide), 17 ft tall, and 75 ft long. The chamber consists of 14 rows (levels) and 20 columns for a total of 280 boards per bay. The bays are paired, with one roll-up door covering two bays. The conversion to CO₂-curing covered one bay. The other half of the paired bay contains the ductwork for CO₂ distribution and is closed off with a blank wall.



Figure 42. Paver and Block Manufacturer #2's curing chambers with roll-down doors

Chamber Preparation and Sealing

The first step in retrofitting the curing chamber was preparing the face of the chamber for accepting a new chamber door. This involved the installation of a custom doorframe to mate with a newly designed door.

Once the new doorframe was mounted on the chamber face, the existing polystyrene insulation inside the chamber was replaced with magnesium oxide board to create a stronger interior surface (**Figure 43**). The chamber interior was then media blasted to clean and roughen the surface (**Figure 44**). Finally, the interior surface was coated with Rhinoliner™ to prevent gas leaks and maintain a secure CO₂ environment within the chamber (**Figure 45**).

The process of sealing the chamber proved to be one of the most challenging and time consuming aspects of the project. Many leak tests and inspections had to be carried out with corrective actions being implemented after each test.



Figure 43. Magnesium oxide board installation



Figure 44. Sandblasting



Figure 45. Spray coating

Door Fabrication and Installation

Solidia collaborated with CDS to design, fabricate and install a chamber door to be used at Paver and Block Manufacturer #2's facility. The finished chamber door is shown in **Figure 46**. Angled guides and rollers were attached to the sides of the door, allowing the weight of the door to provide the necessary force to create the gas-tight seal. A silicone gasket was used around the frame of the door, which contacts the doorframe mounted on the front face of the curing chamber.

A door manipulation device was installed on rails above the curing chamber. This device, shown in **Figure 47**, lowers the door to close and seal the chamber, and raises the door to open the chamber. When the chamber is opened, the rail system is able to move the door to a docking station on the side of the chamber. The operation of the door manipulation device is illustrated in **Figure 48**.



Figure 46.
Completed door



Figure 47.
Door carriage installed

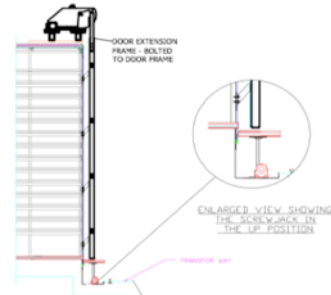


Figure 48.
Door manipulation design

Gas Flow and Distribution Within the Curing Chamber

To assure successful CO₂-curing on an industrial scale, temperature and relative humidity must be recreated within and throughout a commercial curing chamber. To accomplish this, Solidia teamed with Alden Labs to design gas flow and distribution systems for CO₂-curing chambers. Alden's expertise lies in designing complex gas flow systems using Computational Fluid Dynamic (CFD) modeling.

Figure 49 shows two-dimensional “slices” of the CFD model prepared for the chamber conversion at U.S.-based Paver and Block Manufacturer's facility. Note that the gas flow in this chamber runs across the chamber width.

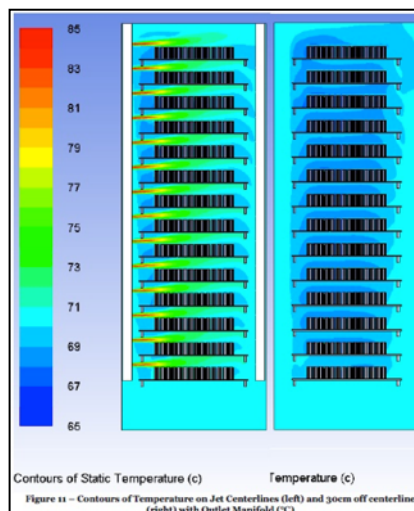


Figure 49. CFD model for Paver and Block Manufacturer #2

Ductwork Design and Installation

As per the CFD modeling, interior ductwork for Paver and Block Manufacturer #2's curing chamber was designed and installed. Large cross-section ducts, for inlet and outlet gas flow, were installed along the length of the chamber. Vertical sections were added to the inlet ducting to direct gas flow over each row of product. These vertical sections are required for each column throughout the length of the chamber. For the outlet ducting, verticals are not required. Rather, larger diameter openings are distributed throughout the outlet ducting length, along the bottom of the chamber.

Figures 50 and 51 below show the ductwork installed on-site in Paver and Block Manufacturer #2's curing chamber. The vertical sections of the inlet ductwork shown in **Figure 50** were installed within the open center rack that separates the two sides of the double bay. The inlet and outlet distribution ducts shown in **Figure 50** were installed in the empty half of the double bay.



Figure 50. Vertical inlet ductwork installed



Figure 51. Inlet and outlet headers installed

Gas Conditioning System Design and Installation

Solidia and Linde, an industrial gas company and supplier of industrial grade CO₂, collaborated to design and build energy-efficient gas conditioning systems for CO₂-curing. The gas conditioning system is composed of a heat exchanger/condenser, a heating system and a blower. The system feeds warm, dry CO₂ into the inlet duct of the curing chamber and receives moist CO₂ from the outlet duct. During the initial curing stages, pure CO₂ is introduced into the curing chamber at relatively high flow rates to displace all the air inside the chamber. Once the chamber is purged, the inlet flow rate is reduced to a level that maintains a high concentration of CO₂ in the chamber. The equipment was specifically sized for use at U.S.-based Paver and Block Manufacturer.

Figures 52 through 54 show different stages of the Gas Conditioning System installation. **Figure 52** shows the heater installed in its final location. **Figure 53** shows the completed Gas Conditioning System from the heater's location. In this photograph, the heater is in the center-foreground, and the heat exchanger is located to the left, behind the heater. **Figure 54** shows the opposite end of the Gas Conditioning System. The main blower is located at the lower left, while the heat exchanger is again located at the rear on the right.



Figure 52. Gas conditioning system - heater



Figure 53. Gas conditioning system - view from heater



Figure 54. Gas conditioning system - view from side opposite heater



Figure 55. Temporary CO₂ tank

Other Site Preparation

A temporary, 26-ton CO₂ tank, acquired from Air Liquide (Figure 55), and a silo dedicated to Solidia Cement (Figure 56) were installed at Paver and Block Manufacturer #2's facility. The auger leaving the cement silo was tied into an existing screw, allowing for minimally invasive operation.

Figure 56. Solidia Cement silo installed (on left)



Paver Curing Equipment Commissioning

The first stage of the Equipment Commissioning phase was to test the gas conditioning equipment's individual system components and their operating range. All components were verified as functional within their target operating ranges.

The second stage involved the development of component operational methods that effect control over the key CO₂-curing process parameters (temperature, humidity, CO₂ concentration, mass flow rates). This included developing a process to purge the chamber by replacing air with CO₂ inside the chamber with attention to efficiency and time. A “plug-flow” method was utilized to displace air with heavier CO₂. Operating conditions that avoid gas mixing during the purging stage were identified to maximize gas stratification. This stage also included programming adjustments to the system that ensure proper component sequencing during recipe-based operation.

The third stage required the chamber to be fully loaded with products for the purpose of validating the uniformity of gas composition inside the chamber during normal production. The chamber was fully loaded during this stage with 280 boards holding 8,400 pavers weighing a total of 43,400 kg, approximately 6,580 kg of this weight being water (**Figures 57 and 58**). In addition to characterizing uniformity in the system, filling the chamber to capacity was required to simulate a full load on the system's components, ensuring that control set points could be achieved.



Figure 57. Commissioning Run #1 production line



Figure 58. Chamber loading

In order to measure uniformity inside the chamber, iButton® sensors were used to record the local temperature and relative humidity at strategically placed locations throughout the chamber, over time. Data from iButton® sensors was then compiled and graphed to visually display the uniformity in the system at a given set-point and time (**Figures 59 and 60**). Pavers from these locations were also measured for residual water, color value, and compressive strength.

Chamber profiles verified that the modeling and ductwork design provided for a CO₂ curing environment within the targeted range of uniformity. At normal operating conditions, maximum temperature and humidity gradients of 10°C and 10%RH respectively were measured inside the chamber.

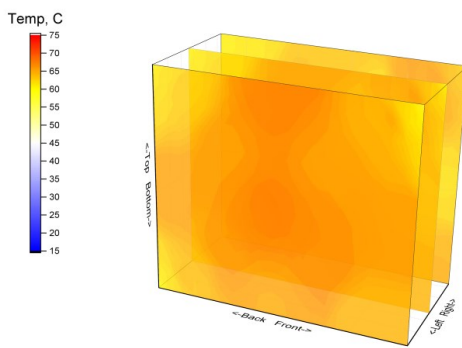


Figure 59. Chamber temperature profile

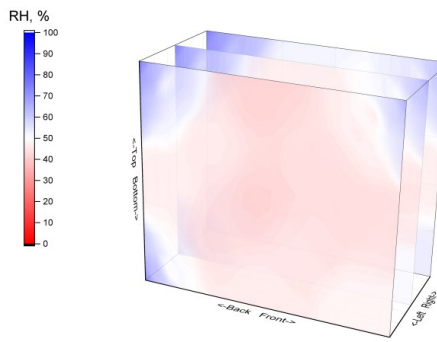


Figure 60: Chamber RH profile

Paver Product Commissioning

While Paver and Block Manufacturer #2 produces a wide range of paver types, two main product types were chosen for commissioning and initial market launch. The goal of the Product Commissioning stage was to refine product formulations and CO₂ curing recipes to be used for regular production with attention to cost, aesthetics, performance, and processing efficiencies.

Existing product formulations were used as a starting point when developing formulations for Solidia Cement-based products to be used at Paver and Block Manufacturer #2. A one-to-one replacement of cementitious material (Cement + Fly ash) to Solidia Cement was used for the Product Commissioning runs.

During the first few concrete batches feeding Commissioning Run #1, paver moisture content and machine settings were dialed-in to achieve a formable and aesthetically acceptable product. These conditions were recorded to set future production parameters. After Commissioning Run #1's curing cycle was complete (20hr), product was unloaded from the chamber. Samples from predetermined boards were removed during this unloading stage; all additional products were palletized and placed in product inventory.

Compressive testing results for products made during Commissioning Run #1 can be seen in **Table 20**. This compressive testing was performed in compliance with ASTM C-936, which states that average compressive strength must be greater than or equal to 8,000 psi with no samples less than 7,200 psi.

Table 20. Compressive Strength Results for Pavers Produced During Commissioning Run #1

Commissioning Run #1	Average	Minimum	Maximum	Standard Deviation
Compressive Strength (psi)	9,651	8,399	11,854	831

* Values represent a sample size of 20 pavers

Testing during this Commissioning Run verified that Solidia Cement-based products at Paver and Block Manufacturer #2 are able to meet compressive strength specifications. The stored carbon content for the pavers made during this commissioning stage was measured at 23.6% of the cement mass in the concrete product.

Solidia Cement-based products from U.S.-based Paver and Block Manufacturer will reach the marketplace and see actual service beginning in June, 2016.

5. Greenhouse Gas and non-GHG Impacts

GHG Benefits Associated with Solidia Cement and Solidia Concrete

Concrete is the world's second most utilized substance, exceeded only by the consumption of water. Over 30 billion tonnes of concrete, containing approximately three billion tonnes of Portland cement, are manufactured and used every year. According to a 2005 study by the World Resources Institute on greenhouse gas emissions by major industries, the cement industry is responsible for 3.8% of the total global greenhouse gas emissions, which is equivalent to 5-7% of industrial CO₂ emissions (from WRI 2005, Navigating the Numbers. Greenhouse Gas Data and International Climate Policy, World Resources Institute. ISBN 1-56973-599-9). Other studies show that the cement industry accounts for about 5% of global anthropogenic carbon dioxide emissions (About Cement, World Business Council for Sustainable Development Cement Sustainability Initiative). According to the International Energy Agency, the cement industry must reduce CO₂ emissions by 66% in order to help limit global temperature rise to 2-3°C by 2050 (www.wbcsdcement.org/pdf/technology/WBCSDIEA_Cement%20Roadmap_centre_spread_actual_size.pdf, and; <http://www.cement.ca/en/Contact-Us.html>).

Though current industry strategies, which include the use of energy-efficient process technologies, alternative fuels, and supplementary cementitious materials, may help reduce emissions moderately, there is a clear need for a transformative innovation.

Solidia Technologies' patented cement chemistry and concrete curing processes offer the building materials and construction industries the ability to manufacture cement and concrete products within existing plants and use traditional design specifications to meet the IEA's CO₂ emissions reduction goal, with minimal requirements for new supply chains and capital investment.

Solidia Cement is composed of a family of "green," low-lime calcium silicate phases, similar, but not identical to the chemistry of Portland cement. As a result, it can be produced in existing cement kilns using the same raw materials that are used to make Portland cement, albeit in different proportions. Solidia Cement is produced using less limestone and at lower temperatures than are necessary for Portland cement. These factors translate into a reduction in the CO₂ emissions during cement manufacturing, from 816 kg per tonne of Portland cement clinker to 570 kg per tonne of Solidia Cement clinker (~30% reduction). This value was demonstrated in March 2014 at the Solidia Cement production trial at the LafargeHolcim cement plant in Whitehall, PA.

To create Solidia Concrete products, water, aggregates and Solidia Cement are mixed, formed into the desired shape and then reacted with gaseous CO₂ to produce a durable binding matrix. The curing process sequesters up to 300 kg of CO₂ per tonne of cement used.

CO₂ Stored in Pavers Cure at Paver and Block Manufacturer #2

In order to calculate the amount of CO₂ stored within a paver produced at the Paver and Block Manufacturer #2's New Jersey plant, core samples with a diameter of 2" were drilled from the cured pavers. These samples were oven dried at 105°C for 72 hours to remove any residual moisture, and placed in a furnace at 550°C for 4 hours to remove any remaining bound water or organic material. Once fully dried, the samples were heated to 950°C at a ramp up rate of 10°C/min. After 3 hours at 950°C, the samples were returned to 105°C and mass loss was recorded. This mass loss was then corrected to account for mass loss from the aggregates.

The remaining mass difference represents the amount of CO₂ sequestered during the curing process and is attributed to the thermal decomposition of CaCO₃ which is the primary reaction product of Solidia Cement carbonation.

A schematic of the process described above is shown in **Figure 61**.

The amount of CO₂ sequestered per paver as measured by Loss on Ignition (LOI) is shown in **Table 21**. The average CO₂ uptake as a % CO₂ by mass of concrete is seen to be 3.50%. **This translates to 471 lbs (213.6kg) of CO₂ being sequestered for every ton of Solidia Cement used in a paver (23.55% CO₂ by mass of cement).**

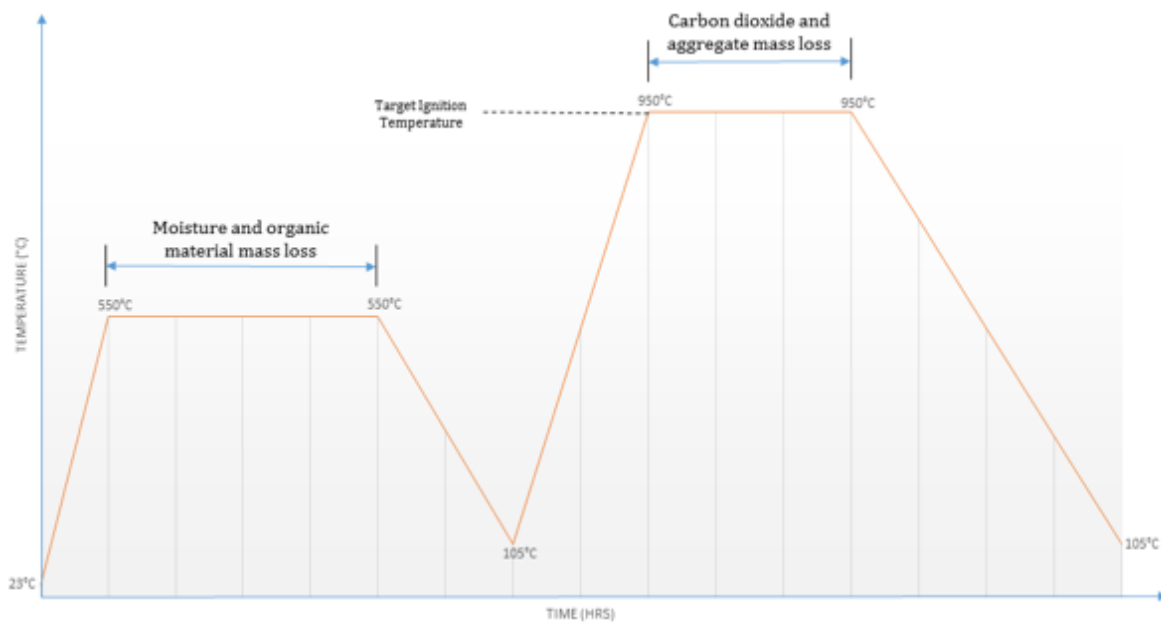


Figure 61. Schematic of the loss on ignition process used to measure CO₂ sequestration in a paver

Table 21. Hollow Core CO₂ sequestration measured by Loss on Ignition (LOI)

Sample #	Loss on Ignition		CO ₂ Uptake		
	Sample Mass Loss 550-950°C (g)	Aggregate Mass Loss 550-950°C (g)	Corrected CO ₂ Uptake (g)	% CO ₂ by mass of concrete	% CO ₂ by mass of cement
1	62.24	45.69	16.555	4.39%	29.53%
2	60.02	45.33	14.686	3.92%	26.40%
3	58.98	46.75	12.229	3.18%	21.32%
4	57.19	45.45	11.736	3.13%	21.04%
5	55.22	43.51	11.713	3.26%	21.94%
6	60.27	45.89	14.383	3.79%	25.54%
7	57.13	44.47	12.661	3.44%	23.20%
8	56.80	44.06	12.745	3.50%	23.58%
9	59.42	45.86	13.557	3.58%	24.09%
10	59.93	46.72	13.206	3.42%	23.03%
11	58.65	46.22	12.433	3.26%	21.92%
12	57.24	45.77	11.471	3.04%	20.42%
13	59.91	44.25	15.660	4.28%	28.84%
14	57.80	44.24	13.562	3.71%	24.98%
15	59.60	47.11	12.488	3.22%	21.60%
16	57.26	46.30	10.959	2.88%	19.29%
		Average	3.50%	23.55%	
		Std Dev.	0.004	0.028	

Table 22 provides the calculated CO₂ footprint reduction associated with the conversion from Portland cement to Solidia Cement at Paver and Block Manufacturer #2's New Jersey plant. The table breaks down the CO₂ footprint reduction into the reduction in CO₂ emissions during cement manufacturing and the CO₂ captured during the curing of concrete products.

For the purposes of this analysis, it will be assumed that Solidia Cement will replace Portland cement on a 1:1 basis by weight. Thus, Paver and Block Manufacturer #2's New Jersey plant will consume 25,000 tons of either Portland cement or Solidia Cement (**Table 22**, line a).

The production of one ton of traditional Portland cement clinker involves the release of about 0.81 tons of CO₂. Approximately two-thirds of the CO₂ emissions can be traced to the chemical decomposition of limestone, while the remainder is emitted from the combustion of fossil fuel used to heat the kiln to 1450°C. The low lime content and reduced kiln temperatures associated with Solidia Cement production enables both the CO₂ released through the decomposition of limestone and the CO₂ emitted from the combustion of fuel to be reduced by 30%. In this manner, CO₂ emissions at a cement plant can be reduced from 0.816 tons of CO₂ per ton of Portland cement clinker to 0.57 tons of CO₂ per ton of Solidia Cement clinker (line b). Thus, CO₂ emissions at the cement plant are reduced by 0.25 tons per ton of cement clinker produced (line c).

By converting Paver and Block Manufacturer #2's New Jersey plant to Solidia Cement, CO₂ emissions at the cement plant are reduced by 6,125 tons (line j = line a x line c).

Portland cement concrete and Solidia Concrete can both be cured and hardened in similar enclosures or chambers. The primary difference is that Portland cement concrete is typically cured in a steam environment while Solidia Concrete is cured in a warm, CO₂-rich environment. It is assumed that the energies associated with the steam curing and CO₂-curing processes are equivalent.

Solidia Concrete will capture and store approximately 0.236 tons of CO₂ per ton of Solidia Cement used in the concrete formulation (line d). The CO₂-curing process will also vent approximately 0.03 tons of CO₂ into the atmosphere per ton of Solidia Cement used in the concrete (line e). In total, 0.266 tons of CO₂ are required to cure Solidia Concrete containing one ton of Solidia Cement (line f).

The CO₂ used in the Solidia Concrete curing process is industrial-grade CO₂ sourced from industrial waste flue gas streams. This CO₂ must be collected at the flue gas site, purified, liquefied, and transported to the concrete manufacturer. Linde, a supplier of industrial grade CO₂, calculates the total average CO₂ emission associated with these operations to be about 0.9 lbs CO₂ per Nm³ product, or ~0.2 lbs./lbs. CO₂ product delivered. Thus, the "current CO₂ cost" associated with Solidia Concrete curing is calculated to be 0.0532 tons of CO₂ per ton of Solidia Cement (line g = 0.2 x line f).

Thus, the net CO₂ captured and stored during the curing of Solidia Concrete is 0.1828 tons per ton of cement today (line h = line d - line g).

By converting Paver and Block Manufacturer #2's New Jersey plant to Solidia Cement, the net CO₂ captured at the concrete plant is 4,570 tons (line k = line a x line h).

In total, the reduction in CO₂ footprint associated with converting Paver and Block Manufacturer #2's New Jersey plant from Portland cement to Solidia Cement is 10,695 tons (line m = line j + line k).

All carbon emission numbers were calculated using 2011 EPA standards and EIA.gov standards.

Table 22. Carbon footprint for Paver and Block Manufacturer #2 for Solidia Cement and Solidia Concrete compared to Portland cement and concrete

		Formula	Unit	Paver and Block Manufacturer #2 Plant			
				SC Concrete (NJ Plant)	OPC Concrete (NJ Plant)		
General Product Specifications							
a	Cement consumed at NJ plant		tons	25000	25000		
Cement Production CO₂ Footprint							
b	CO ₂ emitted during production of one ton Clinker ^a		tons	0.57	0.81		
c	CO ₂ saved/ton SC Clinker ^b		tons	0.25	0		
Concrete Curing CO₂ Footprint (per ton of cement used in concrete)							
d	CO ₂ Sequestered		tons	0.236	0		
e	CO ₂ waste		tons	0.03	0		
f	Total CO ₂ Used	d + e	tons	0.266	0		
g	CO ₂ "Cost" (current state)	f * 0.20 ^c	tons	0.0532	0		
h	Net CO ₂ Sequestered during Curing (current state)	d - g	tons	0.1828	0		
CO₂ Saved using Solidia Technology							
j	CO ₂ saved during cement production	a * c	tons	6125	0		
k	CO ₂ captured during curing	a * h	tons	4570	0		
m	total CO ₂ saved	j + k	tons	10695	0		
CO₂ Footprint Reduction							
n	CO ₂ Footprint reduction (current state)		tons	52.8%	N/A		

Footnotes:

- a. From LafargeHolcim
- b. Trials conducted at Lafarge Whitehall indicate that Solidia Cement (SC) clinker can be produced in a cement kiln while emitting 31% less CO₂ when compared to the production of OPC clinker. It is assumed that all other energy costs associated with the production of the final cement product are equivalent for SC and OPC.
- c. Linde has performed detailed CO₂ footprint analysis for its plants in the US. The analysis includes raw gas purification, compression, liquefaction and transport via trucks or rail cars to customer sites. The total average CO₂ emission associated with the various operations is about 0.9 lbs CO₂ per Nm³ product, or ~0.2 lbs/lbs CO₂ product delivered.

O₂ per Nm³ product, or ~0.2 lbs/lbs CO₂ product delivered.

CO₂ Footprint Reduction Opportunity in the US

The successful completion of the Demonstration of Commercial Application clearly demonstrated the environmental benefits associated with Solidia Cement and Solidia Concrete technologies. The industrial production of Solidia Cement, as a low-lime alternative to traditional Portland cement, reduces CO₂ emissions at the cement kiln from 816 kg of CO₂ per tonne of Portland cement clinker to 570 kg per tonne of Solidia Cement clinker. Industrial scale CO₂-curing of Solidia Concrete, as demonstrated in Subtask 4.3, sequestered a net of 183 kg of CO₂ per tonne of Solidia Cement used in concrete pavers. Taken together, these two effects reduced the CO₂ footprint associated with the production and use of cement in concrete products by over 50% (a reduction of 430 kg of CO₂ per tonne of cement).

Applied at the first commercial Solidia Concrete manufacturing site, the two effects will combine to reduce the CO₂ footprint associated with the production and use of cement by over 10,000 tonnes per year.

When applied across the precast concrete industry in the U.S., it is estimated that the CO₂ footprint will be reduced by 8.6 million tonnes per year (20 million tonnes of cement used in precast concrete x 430 kg of CO₂ per tonne of cement).

Applied across the entire concrete industry in the U.S., it is expected that 43 million tonnes of CO₂ will be avoided per year (100 million tonnes of cement used in all concrete x 430 kg of CO₂ per tonne of cement).

Non-GHG Benefits

Other pollutants associated with cement production, such as mercury, NO_x, and SO_x, are also reduced by conversion from Portland cement to Solidia Cement. Mercury emissions are tied to both limestone consumption and coal consumption. As the requirement for these raw materials are reduced by 30% in Solidia Cement manufacturing, the mercury emissions are reduced by approximately 30%.

Based on the annual cement usage stated above (1,000,000 tonnes in the U.S.), it is estimated that 300,000 tonnes tons of water is chemically consumed annually during concrete production. Another 300,000 tons of water is lost to evaporation during the concrete curing process, which may last up to 28 days. Water is used, but is not consumed, during the Solidia Concrete curing process. It can be collected and reused, with recycle rates in excess of 60%, and potentially as high as 100%.

6. Scientific Achievements

The primary technical achievement associated with the DE-FE0004222 program has been the translation of Solidia Concrete CO₂-curing technology from the laboratory scale to pilot manufacturing scale to full manufacturing scale. Prior to the onset of DE-FE0004222, Solidia Technologies had limited experience in curing large quantities of concrete in non-laboratory environments.

Translating from laboratory scale to full manufacturing scale involved over a hundredfold increase in curing system volume (from ~1 m³ to ~200 m³). Both the concrete mass treated within the curing system and the water removed from the curing atmosphere increased by a factor of eighty (from 0.5 tonne to 40 tonnes of concrete; from 0.2 tonne to 16 tonnes of water).

These jumps required the ability to manufacture and deliver Solidia Cement, to CO₂-cure precast concrete products, and to design the CO₂ gas conditioning and distribution systems capable of maintaining the target CO₂-curing environment (temperature, relative humidity and CO₂ concentration) uniformly throughout industrial-scale curing system volumes, all at scales commensurate with those practiced in the cement and concrete industries.

7. Overall Conclusions

In the course of the DE-FE0004222 program, Solidia Concrete CO₂-curing technology has been successfully translated from laboratory scale to pilot manufacturing scale to full manufacturing scale. This has been demonstrated for a wide variety of precast concrete products. This translation has allowed verification of the following attributes of Solidia Concrete products and of Solidia Concrete manufacturing:

- Solidia Concrete products permanently and safely store significant quantities of CO₂, equal to over 20% of the cement mass used in the concrete.
- Solidia Concrete products meet basic ASTM standards and appeared poised for acceptance by the concrete marketplace.
- Solidia Concrete products offer a number of attractive manufacturing economies when compared to their Portland cement based counterparts. These include reduced raw materials waste, reduced dependence on admixtures to control efflorescence, shorter curing time to full concrete strength, faster equipment clean-up, reduced equipment maintenance, and improved inventory management. These economies more than offset the need to purchase CO₂, and retrofit curing systems to handle CO₂.

The result has been considerable interest among precast concrete manufacturers across the U.S. Potential adopters include a significant portion of the U.S. precast concrete manufacturing industry. Early adopters are likely to be concrete paver, concrete masonry unit, hollow core slab, railroad tie, architectural panel and aerated concrete manufacturers. ***It is important to note that no environmental incentives have been required to attract this commercial interest.***

Solidia Technologies is now poised to transfer CO₂-curing technology to concrete manufacturers to enable the realization of the benefits described above. To accomplish this task, two strategic partners will provide critical support:

- LafargeHolcim is one of the world's largest producers of cement, and is also a manufacturer of precast concrete products. As a result, they are positioned to be both the initial supplier of Solidia Cement and a launch customer of Solidia Cement, in Canada and worldwide. ***Of importance to the the DE-FE0004222 program, LafargeHolcim operates six cement manufacturing plants in the U.S.*** With an existing marketing and sales team that spans the globe, LafargeHolcim will also serve as the Solidia Cement point of contact with the concrete industry.
- Air Liquide is a world leader in industrial gases and related technologies. As a primary producer of industrial grade CO₂ in Canada and worldwide, Air Liquide will provide CO₂ gas and is capable of providing gas handling expertise to Solidia Cement customers. In addition, they will design and construct the equipment needed to retrofit a concrete manufacturer's curing system to allow CO₂-curing.

The primary, unanswered question at this point in time involves the use of Solidia Cement and CO₂-curing in cast-in-place concrete applications. Penetration of the cast-in-place market is necessary to reach the full environmental benefit of the Solidia Cement / Solidia Concrete technologies. This will be one of the topics addressed in future Solidia Technologies research programs.

Together, Solidia Technologies, LafargeHolcim and Air Liquide are capable of enabling the adoption of CO₂-curing technology throughout the U.S., allowing the cement and concrete industries the opportunity to reduce their collective CO₂ footprint by between 8.6 million tonnes per year (with the conversion of the precast concrete market) and 43 million tonnes (with the conversion of the entire concrete market).